AD-A080 965 TETRA TECH INC PASADENA CALIF F/G 20/4
PARTIALLY CAVITATING CASCADE THEORIES AND THEIR APPLICATION TO --ETC(U)
OCT 79 O FURUYA, S MAEKAWA N00014-79-C-0234
UNCLASSIFIED TETRAT-TC-3284-01 NL

END
DATE FILMED
2-80
DDC

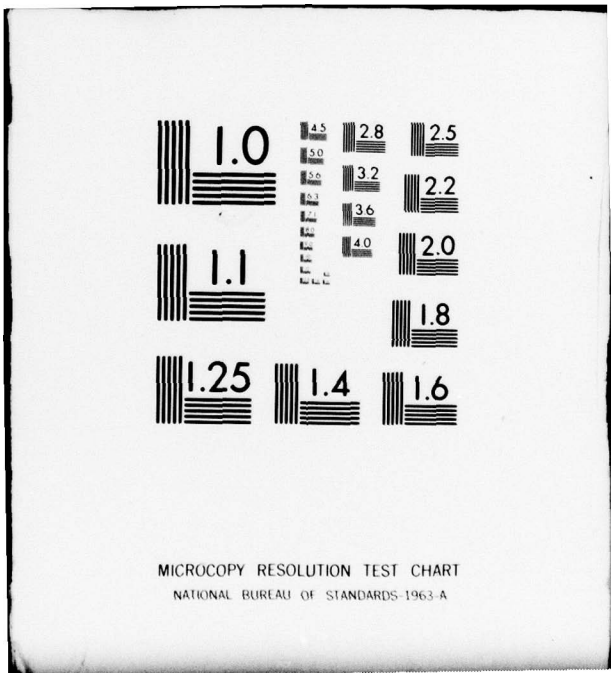
1.0
1.1
1.25
1.4
1.6
1.8
2.0
2.2
2.5
2.8
3.2
3.6
4.0
4.5
5.0
5.6
MICROCOPY RESOLUTION TEST CHART
NATIONAL BUREAU OF STANDARDS-1963-A

(1) LEVEL II

Report No. TC 3284-01
Contract No. N00014-79-C-0234 (GHR PROGRAM)

PARTIALLY CAVITATING CASCADE THEORIES AND THEIR APPLICATION TO CAVITATING PROPELLER FLOWS

By

OKITSUGU FURUYA
SHIN MAEKAWA

TETRA TECH, INC.
630 NORTH ROSEMEAD BOULEVARD
PASADENA, CALIFORNIA 91107

OCTOBER 1979

Prepared for
DAVID W. TAYLOR NAVAL SHIP R&D CENTER
BETHESDA, MARYLAND 20084

OFFICE OF NAVAL RESEARCH
800 NORTH QUINCY STREET
ARLINGTON, VIRGINIA 22217

Approved for public release;
distribution unlimited

Report No. TC 3284-01
Contract No. N00014-79-C-0234 (GHR PROGRAM)

PARTIALLY CAVITATING CASCADE THEORIES AND THEIR APPLICATION TO CAVITATING PROPELLER FLOWS

By

OKITSUGU FURUYA
SHIN MAEKAWA

TETRA TECH, INC.
630 NORTH ROSEMEAD BOULEVARD
PASADENA, CALIFORNIA 91107

OCTOBER 1979

This research was carried out under the Naval Sea Systems Command General Hydromechanics Research Program Subproject SR 023 01 01, administered by the David W. Taylor Naval Ship Research and Development Center, Contract N00014-79-C-0234.

Prepared for
DAVID W. TAYLOR NAVAL SHIP R&D CENTER
BETHESDA, MARYLAND 20084

OFFICE OF NAVAL RESEARCH
800 NORTH QUINCY STREET
ARLINGTON, VIRGINIA 22217

UNCLASSIFIED

SECURITY CLASSIFICATION OF THIS PAGE (When Data Entered)

REPORT DOCUMENTATION PAGE

READ INSTRUCTIONS BEFORE COMPLETING FORM

1. REPORT NUMBER: TC 3284-01
2. GOVT ACCESSION NO.:
3. RECIPIENT'S CATALOG NUMBER:

4. TITLE (and Subtitle): (6) PARTIALLY CAVITATING CASCADE THEORIES AND THEIR APPLICATION TO CAVITATING PROPELLER FLOWS
5. TYPE OF REPORT & PERIOD COVERED: Technical-Theory, Feb. 15, 1979-Oct. 31, 1979
6. PERFORMING ORG. REPORT NUMBER: TC 3284-01

7. AUTHOR(s): (10) Okitsugu Furuya, Shin Maekawa
8. CONTRACT OR GRANT NUMBER(s): (15) N00014-79-C-0234

9. PERFORMING ORGANIZATION NAME AND ADDRESS: TETRA TECH, INC., 630 North Rosemead Blvd. (12) 66, Pasadena, CA 91107
10. PROGRAM ELEMENT, PROJECT, TASK AREA & WORK UNIT NUMBERS: DWTNSR&DC 9191967/10-30-78(1505)

11. CONTROLLING OFFICE NAME AND ADDRESS: David W. Taylor Naval Ship R&D Center, Department of the Navy, Bethesda, Maryland 20084 (11)
12. REPORT DATE: Oct [redacted] 79
13. NUMBER OF PAGES: 62

14. MONITORING AGENCY NAME & ADDRESS(if different from Controlling Office): Office of Naval Research, 800 North Quincy Street, Arlington, Virginia 22217
15. SECURITY CLASS. (of this report): Unclassified
15a. DECLASSIFICATION/DOWNGRADING SCHEDULE:

16. DISTRIBUTION STATEMENT (of this Report): Approved for public release; distribution unlimited
(16) SR023 01
(17) SR023 01 01

17. DISTRIBUTION STATEMENT (of the abstract entered in Block 20, if different from Report)
(14) TETRAT-TC-3284-01

18. SUPPLEMENTARY NOTES: Sponsored by the Naval Sea Systems Command General Hydrodynamic Research Program and administered by the David W. Taylor Naval Ship R&D Center, Code 1505, Bethesda, Maryland 20084.

19. KEY WORDS (Continue on reverse side if necessary and identify by block number):
Partial cavity flow
Cascade
Nonlinear theory
Partially cavitating propeller
(9) Technical rept. 15 Feb-31 Oct 79,

20. ABSTRACT (Continue on reverse side if necessary and identify by block number):
In addition to the previously developed partially cavitating cascade theory, two new flow models were constructed in search of a better flow model for determining accurate force coefficients. Effort has been made for obtaining i) physically acceptable flows, particularly the location of cavity boundary and ii) smooth matching of the flow characteristics between the partially cavitating and supercavitating flow regimes. Based on the numerical results made with these flow models for practical blade profiles taken after a supercavitating

DD FORM 1 JAN 73 1473 EDITION OF 1 NOV 65 IS OBSOLETE S/N 0102-014-6601

UNCLASSIFIED 403146

SECURITY CLASSIFICATION OF THIS PAGE (When Data Entered)

20. propeller it was found that no single flow model developed above could handle the complete set of cascade geometries and incidence angles. One theory was supplemental to the other and no definite guideline was discovered for selection of an appropriate flow model for a specified flow condition to be solved except for a few weak evidences. The data calculated with one of the above theories were used in the high speed propeller theory for predicting the performance of a supercavitating propeller operating at the partially cavitating regime. The results showed a slight improvement over the previous ones, indicating a good possibility of increasing the prediction capability of the propeller theory for the partial cavitating flow regime. In doing this, a more accurate theory will have to be developed. Before making further effort on developing such a theory, many unknown aspects regarding the boundary condition of the partially cavitating cascade flow should be clarified. A systematic experimental study for such flow is now in order and strongly recommended.

TABLE OF CONTENTS

		Page
	NOMENCLATURES	ii
I.	SUMMARY	v
II.	ACKNOWLEDGMENTS	vi
III.	LIST OF FIGURES AND TABLES	vii
1.	INTRODUCTION	1
2.	MODIFICATION OF PARTIALLY CAVITATING (p/c) CASCADE THEORY FOR CAMBERED FOILS	4
	2.1 THEORY	4
	2.2 NUMERICAL RESULTS WITH THE NEW THEORY	12
	2.3 APPLICATION OF THE NEW p/c CASCADE DATA TO A CAVITATING PROPELLER	14
3.	DOUBLE WAKE MODEL FOR p/c CASCADE FLOWS	16
	3.1 THEORY	16
	3.2 NUMERICAL RESULTS	24
4.	SUMMARY AND RECOMMENDATION	26
5.	REFERENCES	30

NOMENCLATURES

$\tilde{A}$	scale factor for mapping between W and ζ planes
b	ξ-coordinate corresponding to the upper cavity separation point
c	ξ-coordinate corresponding to the cavity reattachment position and also used as a chord length of blade
C_L, C_D	lift and drag coefficients parallel and normal to the incoming flow direction $\left(= L \text{ or } D/\frac{1}{2}\rho U_1^2 c\right)$
$\bar{C}_L, \bar{C}_D$	lift and drag coefficients in the direction of the x and y axes
C_{Lm}	lift coefficients in the x-direction normalized by the geometric mean velocity U_m
C_p	pressure coefficient $\left(= (p-p_1)/\frac{1}{2}\rho U_1^2\right)$
D	drag force
d	spacing of cascade blades
f	ξ-coordinate corresponding to the upper trailing edge or blade profile
f_i	nonlinear equations representing the boundary value problem for the open wake model
f_{iw}	nonlinear equations representing the boundary value problem for the double wake model
g	ξ-coordinate corresponding to the lower end point of near wake
h	ξ-coordinate corresponding to the upper end point of near wake
i	index for complex variable $\left(= \sqrt{-1}\right)$
L	lifting force
ℓ_c	cavity length
p	static pressure
q	flow velocity modulus
S_1, S_2	total arc lengths of the upper and lower wetted part of the blade, respectively

S_t	stagnation point
$s(\xi)$	local arc length measured from either the leading edge or the reattachment point of cavity
$sg(x)$	sign function $\begin{pmatrix} = 1 \text{ for } x \geq 0 \\ = -1 \text{ for } x < 0 \end{pmatrix}$
TH	thickness of plano-convex blade normalized by chord
T	lower trailing edge of blade
U	flow velocity amplitude
W	complex potential $= (\Phi + i\Psi)$
x	horizontal coordinate attached to cascade in physical plane or normalized spanwise location of the propeller blade
y	vertical coordinate attached to cascade in physical plane
z	physical plane $(= x+iy)$
α	flow angle made with the x-axis of the physical plane
β	local blade slope measured from the x-axis, clockwise negative; for the second arc S_2, $-\pi$ is to be added
γ	geometric stagger angle
Γ	circulation around the body
δ	stagger angle of the potential plane cascade set-up $(= \alpha_1 + \gamma)$
ϵ	ratio of the flow path width at upstream to downstream infinity of the cascade $(= d_2/d_1)$
ζ	transform potential plan $(= \xi + i\eta)$
ζ_1	ζ-coordinate corresponding to the upstream infinity of the physical plane
η	vertical coordinate in the ξ-plane
θ	flow angle
ξ	horizontal coordinate in the ζ-plane
σ	cavitation number $\left(= (p_1 - p_c)/\frac{1}{2}\rho U_1^2\right)$
τ	logarithmic velocity normalized by U_2 $\left(= \ell n(q/U_2)\right)$

Φ	potential function
Ψ	stream function
ω	hodograph variable ($= \theta + i\tau$)

Subscripts

1 and 2	denotes quantities belonging to the upstream and downstream infinities, respectively, or quantities belonging to the first and second arcs, respectively
c	denotes the cavity or quantities at the cavity or at the cavity boundary
m	denotes geometric mean quantities
u	denotes upper surface of blade
w	denotes quantites at the first wake or the boundary of the near wake or quantities belonging to the double wake model

Superscripts

+,-,	quantities belonging to the immediate upper and lower sides of the ξ-axis

I. SUMMARY

In addition to the previously developed partially cavitating cascade theory, two new flow models were constructed in search of a better flow model for determining accurate force coefficients. Effort has been made for obtaining i) physically acceptable flows, particularly the location of cavity boundary and ii) smooth matching of the flow characteristics between the partially cavitating and supercavitating flow regimes. Based on the numerical results made with these flow models for practical blade profiles taken after a supercavitating propeller it was found that no single flow model developed above could handle the complete set of cascade geometries and incidence angles. One theory was supplemental to the other and no definite guideline was discovered for selection of an appropriate flow model for a specified flow condition to be solved except for a few weak evidences. The data calculated with one of the above theories were used in the high speed propeller theory for predicting the performance of a supercavitating propeller operating at the partially cavitating regime. The results showed a slight improvement over the previous ones, indicating a good possibility of increasing the prediction capability of the propeller theory for the partial cavitating flow regime. In doing this, a more accurate theory will have to be developed. Before making further effort on developing such a theory, many unknown aspects regarding the boundary condition of the partially cavitating cascade flow should be clarified. A systematic experimental study for such flow is now in order and strongly recommended.

II. ACKNOWLEDGMENTS

This research was carried out under the Naval Sea Systems Command, General Hydromechanics Research Program, administered by the David Taylor Naval Ship Research and Development Center, Contract N00014-79-C-0234. The authors thank Professor Acosta at the California Institute of Technology for his valuable advice and suggestions.

III. LIST OF FIGURES AND TABLES

Figure		Page
2.1	Cavity Boundary Calculated with the Previous P/C Cascade Theory (Furuya 1978) for Hydronautics 7607.02 Propeller Blade Section at 50% Span Position, $\alpha_1 = 4°$ and $\ell_c = .35$.	33
2.2	Schematic Diagram for the New P/C Cascade Flow Model	34
2.3	Cavity Boundary Calculated with the New Flow Model for the Same Blade as that in Figure 2.1	35
2.4	C_L vs. σ at x = .5 of Hydronautics 7607.02 Propeller, the C_L Values being calculated with the New Flow Model.	36
2.5	C_D vs. σ for the Same Blade as that in Figure 2.4	37
2.6	Cavity Length ℓ_c vs. Cavitation Number σ for the Cases of Figure 2.4 and 2.5.	38
2.7	C_L vs. σ at x = .6 of Hydronautics 7607.02 Propeller, the C_L values being calculated with the New Flow Model.	39
2.8	C_D vs. σ for the Same Blade Section as that of Figure 2.7.	40
2.9	Cavity Length ℓ_c vs. Cavitation Number σ for the Cases of Figures 2.7 and 2.8	41
2.10	Locations of the Calculated Cavity Boundaries for the Blade Profile at the Spanwise Position of 50% of Hydronautics 7607.02	42
2.11	The Same as that of Figure 2.10 except that the Spanwise Location is 60%	43
2.12	Comparison of the Present Results for K_T, K_Q and η of Hydronautics 7607.02 at $\sigma_{Va} = .343$ with those of the Previous Theory (Furuya 1978b) and Experiments (Bohn 1977 and Peck 1977	44

Figure		Page
2.13	Propeller Sectional Data for Figure 2.10 Where x Designates the Normalized Spanwise Location. .	45
2.14	The Same as Figure 2.10 except that this is the case for $\sigma_{Va} = 3.0$	46
2.15	Propeller Sectional Data for Figure 2.12	47
3.1	Comparison of the Flow Configuration Between the Partially Cavitating Condition and Supercavitating Condition as the Cavity Length approaches to the Chord Length.	48
3.2(a)	Comparison of the Pressure Distribution of the Pressure Side Between the P/C Cascade Theory (Furuya 1978) and S/C Cascade Theory (Furuya 1975) for the Hydronautics Propeller 7607.02 Section at x = .5 and $\alpha_1 = 8°$.	49
3.2(b)	The Same as Figure 3.2(a) except that these are the cases for $\alpha_1 = 4°$.	50
3.3	Schematic Diagram for the Double Wake Model for the Partially Cavitating Cascade Flow and its Mapping Planes	51
3.4	Lift Coefficient vs. Cavitation Number Calculated with the New Partially Cavitating Cascade Theory in Comparison with the Previous Theory at x = 0.5 for Hydronautics Propeller 7607.02 . . .	52
3.5	Drag Coefficient vs. Cavitation Number for the Same Case as Figure 3.4.	53
3.6	Cavity Length vs. Cavitation Number for the Same Case as Figures 3.5 and 3.6	54

Table		
2.1	Lift and Drag Data Near $\ell_c = 1$ Calculated from the Supercavitating (s/c) Cascade Theory and Partially Cavitating (p/c) Cascade Theory. . . .	31

1. INTRODUCTION

A performance prediction method for cavitating marine propellers has been developed by combining the propeller lifting-line theory with the supercavitating cascade theory (Furuya 1976, 1978b). This method was applied for calculating the performance characteristics of a few supercavitating propellers such as TMB Model 3770 and Hydronautics 7607.02. It was found that the predicted force coefficients with the method compared favorably with their experimental data over a range of the advance speed J for which the supercavitating condition prevails. On the other hand, for larger J's for which the partially cavitating flow appears on a part of or whole propeller blade, the predicted thrust and torque coefficients rapidly departed from those of experiments (see Figures 2.12 and 2.14, reproduced from Furuya 1978b). It was considered that this discrepancy was attributable to the use of the erroneous supercavitating cascade data in the propeller theory for the partially cavitating flow regime.

The objective of the whole project was therefore first to develop the partially cavitating cascade theory and then to incorporate the data calculated with such theory into high-speed propeller theory. During the initial phase under the GHR project the backbone for the partially cavitating cascade theory was established (Furuya 1978). Computer programs (PCAS and PCASL) developed based on the above mathematical formulation were applied to a cascade of plano-convex blades with various blade thickness. Representative numerical calculations made with these programs showed a good agreement with experimental data of Wade and Acosta (1967).

The remaining tasks for the present phase were to generate sectional data for practical blade profiles of a supercavitating propeller with the previously developed cascade theory

and then to use such data in the propeller program for predicting the propeller performance operating under the partially cavitating regime. When the blade sectional profile of Hydronautics 7607.02 supercavitating propeller, having rather large camber, was used in PCAS and PCASL, a problem of the calculated upper cavity boundary crossing the blade surface, which is physically not acceptable, arose. This was not surprising since the flow model used here had no control on the location of the cavity closure point and this type of problem is quite commonly experienced in supercavitating blade design procedure (see, e.g. Yim and Higgins (1975)). In order to overcome this problem we developed a new flow model for the partially cavitating cascade flow in which the boundary condition for the cavity end point to stay on the upper blade surface was added but with allowing the wake to open at downstream infinity. In the following section the theory formulation for this new flow model and computation for the sectional blade profiles of Hydronautics 7607.02 propeller as well as the application of the data obtained there for the propeller theory will be described in detail.

As will be seen in Section 2, this new flow model was found to be not quite satisfactory in accuracy for the data obtained. The lift and drag forces calculated from this partially cavitating cascade theory sometimes matched smoothly with those of the supercavitating cascade theory as ℓ_c/c approached unity, but sometimes not, depending upon the cascade geometry and incidence angle. It was discovered that this mismatching was particularly eminent for rather small incidence angle cases. Close investigations on the flow models used for both supercavitating (s/c) and partially cavitating (p/c) theories as well as the calculated results revealed two possible reasons for the discrepancy. First, the base pressure between the s/c and p/c theories is totally different no matter how closely the length of cavity approaches to that of chord; it is p_c for the former whereas it is p_2 for the latter. Secondly, it was

shown in the results obtained with the s/c theory that the cavity thickness was so thin that it either barely cleared the upper blade surface or crossed it for small incidence angle cases. There exists no remedy for the cavity boundary of the s/c flow crossing the blade surface. It simply means that the data for such cases must be ignored since such flows should not physically exist.

For a further improvement on the partially cavitating cascade theory the third flow model, i.e., "double wake" model, was introduced here. In this flow model, the near wake and far wake, one after another immediately behind the blade having blunt trailing edge, were used in the same way as is observed in the actual wake flow. In choosing the pressure for the near wake, Professor Acosta at the California Institute of Technology suggested a linear interpolation between those inside the cavity and far wake. Although the validity of this interpolation method should await comparison with experimental data, the method at least guarantees the smooth blending of the base pressure between the two flow regimes. In Section 3 this double wake model will be described, followed by representative numerical results.

2. MODIFICATION OF PARTIALLY CAVITATING (p/c) CASCADE THEORY FOR CAMBERED FOILS

2.1 THEORY

The nonlinear theory for partially cavitating cascade flows previously developed (Furuya 1978) was applied to the blade profiles of Hydronautics' 7607.02 propeller. Although convergent solutions were obtained with this theory, we encountered a problem of the cavity end-point crossing the foil upper surface and ending at a physically unacceptable point. Figure 2.1 shows one such example. The blade profile and cascade geometry used for this calculation were those at 50% radial station of 7607.02, incidence angle $\alpha_1 = 4°$ and $\ell_c = .35$. This type of problem is well-known in the design method of supercavitating hydrofoils or cascades (see Yim and Higgins 1975) where the pressure distribution which provides a good lift-to-drag ratio is usually specified and the corresponding foil profile should be determined. In many cases designers will find that the calculated upper cavity boundary crosses over the blade surface.

In order to overcome this problem, a modification has been made on the existing theory (Furuya 1978) and then the computer program; an additional constraint has been placed to force the cavity end-point to close on the upper surface of the foil. Along with this additional boundary condition, a new unknown variable, ε, was introduced to accommodate the additional equation where ε is taken to be the ratio of the blade spacing to the flow width at downstream infinity. It means that with the additional condition forcing the cavity end-point to end on the body boundary it is no longer possible for the wake to close at downstream infinity (see Figure 2.2). This extra condition and unknown parameter therefore will change the flow model from the closed wake model to the open wake model. It is noted that our

open wake model is different from Wu's open wake model (1968) since the pressure inside the wake in this model is a constant everywhere and equal to that of the downstream infinity. Again two types of the boundary value problems, one specifying the cavitation number (computer code "PCASE") and the other specifying the length of cavity (computer code "PCASLE"), were formulated and the computer codes were tested in several cases. Although most of the boundary conditions remain the same as those of the previous theory (Furuya 1978), the new boundary value problem used here will be described in the complete form for a clear understanding of the theory change.

The hodograph variable ω is defined in the same way as before

$$\frac{dW}{dz} = qe^{-i\theta} = U_2 e^{-i\omega} \quad , \tag{2.1}$$

thus

$$\omega = \theta + i\tau \tag{2.2}$$

$$\tau = \ln (q/U_2). \tag{2.3}$$

where W is a complex potential function, $W = \Phi + i\Psi$.

The cascade-mapping function between the W-plane and ζ-plane is

$$W = \frac{d}{2\pi}\left\{e^{-i\delta}\ln\left(1-\frac{\zeta}{\zeta_1}\right) + e^{i\delta}\ln\left(1-\frac{\zeta}{\bar{\zeta}_1}\right)\right\} \tag{2.4}$$

where

$$\zeta_1 = \tilde{A}e^{i(\pi/2-\delta)}$$

$$\delta = \gamma + \alpha_1.$$

The solution form for the hodograph variable ω also remains the same (see Furuya (1978)),

$$\omega(\zeta) = \sqrt{\frac{(\zeta+1)(\zeta-b)(\zeta-f)}{\zeta-c}}\ \frac{1}{2\pi i}\left\{\int_{-1}^{b} \frac{2\beta_1}{i\sqrt{\frac{(\xi'+1)(b-\xi')(\xi'-f)}{\xi'-c}}}\ \frac{d\xi'}{\xi'-\zeta}\right.$$

$$+\int_{0}^{b} \frac{2\pi}{i\sqrt{\frac{(\xi'+1)(b-\xi')(\xi'-f)}{\xi'-c}}}\ \frac{d\xi'}{\xi'-\zeta}$$

$$+\int_{b}^{c} \frac{2i\ \ln\left(\sqrt{1+\sigma}/U_2\right)}{\sqrt{\frac{(\xi'+1)(\xi'-b)(\xi'-f)}{\xi'-c}}}\ \frac{d\xi'}{\xi'-\zeta}$$

$$\left.+\int_{c}^{f} \frac{2\beta_2+2\pi}{\sqrt{\frac{(\xi'+1)(\xi'-b)(f-\xi')}{\xi'-c}}}\ \frac{d\xi'}{\xi'-\zeta}\right. . \qquad (2.5)$$

The unknown parameters in the present problem include U_2, α_2 $\tilde{A}$, b, c, f and ε, requiring seven equations for the unique determination of these parameters. The boundary conditions to be used here are described as follows:

(i) At the upstream infinity, $\omega(\zeta_1) = \alpha_1 + i\ \ell n(1/U_2)$: 2 equations

(ii) At the downstream infinity, $\omega(\infty) = \alpha_2$: 1 equation

(iii) Length of first arc $\equiv S_1$: 1 equation

(iv) End point of the streamline (ξ=f) matches the physical trailing edge: 1 equation

(v) Continuity equation: 1 equation

(vi) Cavity closure condition (on the upper body surface): 1 equation.

Application of these conditions to Equation (2.5) yields the following seven equations:

i) <u>At Upstream Infinity:</u>

$$\left.\begin{Bmatrix} f_1 \\ f_2 \end{Bmatrix} \equiv \sqrt{\frac{(\zeta_1+1)(\zeta_1-b)(\zeta_1-f)}{\zeta_1-c}}\right\} - \frac{1}{\pi}\int_{-1}^{b} \frac{\beta_1}{\sqrt{\frac{(\xi'+1)(b-\xi')(\xi'-f)}{\xi'-c}}} \frac{d\xi'}{\xi'-\zeta_1}$$

$$- \int_{0}^{b} \frac{1}{\sqrt{\frac{(\xi'+1)(b-\xi')(\xi'-f)}{\xi'-c}}} \frac{d\xi'}{\xi'-\zeta_1} + \frac{1}{\pi} \ln\left(\frac{\sqrt{1+\sigma}}{U_2}\right) x$$

$$\left. \int_{b}^{c} \frac{1}{\sqrt{\frac{(\xi'+1)(\xi'-b)(\xi'-f)}{\xi'-c}}} \frac{d\xi'}{\xi'-\zeta_1} - \frac{1}{\pi}\int_{c}^{f} \frac{\beta_2+\pi}{\sqrt{\frac{(\xi'+1)(\xi'-b)(f-\xi')}{\xi'-c}}} \frac{d\xi'}{\xi'-\zeta_1} \right\}$$

$$- \left\{ \alpha_1 + i \ln(1/U_2) \right\} = 0 \qquad (2.6)$$

ii) <u>At Downstream Infinity:</u>

$$f_3 \equiv \frac{1}{\pi}\int_{-1}^{b} \frac{\beta_1}{\sqrt{\frac{(\xi'+1)(b-\xi')(\xi'-f)}{\xi'-c}}} d\xi' + \int_{0}^{b} \frac{d\xi'}{\sqrt{\frac{(\xi'+1)(b-\xi')(\xi'-f)}{\xi'-c}}}$$

$$- \frac{1}{\pi} \ln\left(\frac{\sqrt{1+\sigma}}{U_2}\right) \int_{b}^{c} \frac{d\xi'}{\sqrt{\frac{(\xi'+1)(\xi'-b)(\xi'-f)}{\xi'-c}}} +$$

$$\frac{1}{\pi}\int_{c}^{f} \frac{\beta_2+\pi}{\sqrt{\frac{(\xi'+1)(\xi'-b)(f-\xi)}{\xi'-c}}} d\xi' - \alpha_2 = 0 \qquad (2.7)$$

iii) First Arc Length = S_1:

On the wetted part of the streamline,

$$\frac{dz}{ds_1} = e^{i\beta_1}$$

thus

$$ds_1 = e^{-i\beta}\,\frac{e^{i\omega}}{U_2}\,\frac{dW}{d\xi}\,d\xi\ .$$

For $-1 < \xi < b$, $\omega(\zeta)$ can be written as follows;

$$\omega(\xi) = \begin{cases} ig_1(\xi) + \beta_1(\xi) & , \quad -1 < \xi < 0 \\ ig_1(\xi) + \beta_1(\xi) + \pi, & \quad 0 < \xi < b \end{cases}$$

where

$$g_1(\xi) = \sqrt{\frac{(\xi+1)(b-\xi)(\xi-f)}{\xi-c}} \left\{ -\frac{1}{\pi}\int_{-1}^{b} \frac{\beta_1}{\sqrt{\frac{(\xi'+1)(b-\xi')(\xi'-f)}{\xi'-c}}}\,\frac{d\xi'}{\xi'-\xi} \right.$$

$$-\int_{0}^{b} \frac{1}{\sqrt{\frac{(\xi'+1)(b-\xi')(\xi'-f)}{\xi'-c}}}\,\frac{d\xi'}{\xi'-\xi} + \frac{1}{\pi}\,\ln\left(\frac{\sqrt{1+\sigma}}{U_2}\right) x$$

$$\left. \int_{b}^{c} \frac{1}{\sqrt{\frac{(\xi'+1)(\xi'-b)(\xi'-f)}{\xi'-c}}}\,\frac{d\xi'}{\xi'-\xi} - \frac{1}{\pi}\int_{c}^{f} \frac{\beta_2+\pi}{\sqrt{\frac{(\xi'+1)(\xi'-b)(f-\xi')}{\xi'-c}}}\,\frac{d\xi'}{\xi'-\xi} \right\} . \quad (2.8)$$

After integrating the above equation, one finds;

$$s_1(\xi) = \int_{\xi}^{b} sg(\xi)\,\frac{e^{-g_1(\xi)}}{U_2}\,\frac{dW}{d\xi}\,d\xi$$

where

$$sg(\xi) = \begin{cases} 1 & , \quad \xi > 0 \\ -1 & , \quad \xi < 0 . \end{cases}$$

The arc length condition is therefore satisfied by the following equation;

$$f_4 \equiv S_1 - s_1(-1) = 0 \tag{2.9}$$

where $dW/d\xi$ is given by Equation (4).

iv) <u>End Point of the Streamline at $\xi = f$ Matching the Trailing Edge of the Blade</u>:

Similar to the above derivation, the equation f_5 is obtained as follows:

$$f_5 \equiv S_2 - s_2(f) = 0 \tag{2.10}$$

where

$$s_2(\xi) = \int_c^{\xi} \frac{e^{-g_2(\xi)}}{U_2} \frac{dW}{d\xi'} d\xi'$$

and

$$g_2(\xi) = \sqrt{\frac{(\xi+1)(\xi-b)(f-\xi)}{\xi-c}} \left\{ - \frac{1}{\pi} \int_{-1}^{b} \frac{\beta_1}{\sqrt{\frac{(\xi'+1)(b-\xi')(\xi'-f)}{\xi'-c}}} \frac{d\xi'}{\xi'-\xi} \right.$$

$$- \int_0^b \frac{1}{\sqrt{\frac{(\xi'+1)(b-\xi')(\xi'-f)}{\xi'-c}}} \frac{d\xi'}{\xi'-\xi} + \frac{1}{\pi} \ln \left(\frac{\sqrt{1+\sigma}}{U_2} \right) x$$

$$\left. \int_b^c \frac{1}{\sqrt{\frac{(\xi'+1)(\xi'-b)(\xi'-f)}{\xi'-c}}} \frac{d\xi'}{\xi'-\xi} - \frac{1}{\pi} \int_c^f \frac{\beta_2+\pi}{\sqrt{\frac{(\xi'+1)(\xi'-b)(f-\xi')}{\xi'-c}}} \frac{d\xi'}{\xi'-\xi} \right\} \tag{2.11}$$

In order to determine the second arc length S_2, the end point of cavity should be known. The cavity shape is expressed in terms of ξ-coordinate;

$$x-x_B = \frac{1}{\sqrt{1+\sigma}} \int_b^{\xi} \cos g_c(\xi') \frac{dW}{d\xi'} d\xi' \tag{2.13}$$

$$y-y_B = \frac{1}{\sqrt{1+\sigma}} \int_b^{\xi} \sin g_c(\xi') \frac{dW}{d\xi'} d\xi' \tag{2.14}$$

where

$$g_c(\xi) = \sqrt{\frac{(\xi+1)(\xi-b)(f-\xi)}{c-\xi}} \left\{ -\frac{1}{\pi} \int_{-1}^{b} \frac{\beta_1(\xi')}{\sqrt{\frac{(\xi'+1)(b-\xi')(\xi'-f)}{\xi'-c}}} \frac{d\xi'}{\xi'-\xi} \right.$$

$$-\int_{o}^{b} \frac{1}{\sqrt{\frac{(\xi'+1)(b-\xi')(\xi'-f)}{\xi'-c}}} \frac{d\xi'}{\xi'-\xi} + \frac{1}{\pi} \ln\left(\frac{\sqrt{1+\sigma}}{U_2}\right) \times$$

$$\left. \int_{b}^{c} \frac{1}{\sqrt{\frac{(\xi'+1)(\xi'-b)(\xi'-f)}{\xi'-c}}} \frac{d\xi'}{\xi'-\xi} - \frac{1}{\pi} \int_{c}^{f} \frac{\beta_2+\pi}{\sqrt{\frac{(\xi'+1)(\xi'-b)(f-\xi')}{\xi'-c}}} \frac{d\xi'}{\xi'-\xi} \right\} . \tag{2.15}$$

x_B, y_B are the physical coordinates of the blade leading edge. The end point of the cavity (x_c, y_c) is obtained by setting the upper bound of the above integrals (2.13) and (2.14) to be c. Once (x_c,y_c) are determined, the second arc length S_2 is readily calculated by following the body profile.

v) Continuity Equation

The continuity equation applied here at upstream and downstream infinities becomes

$$f_6 \equiv U_1 \cos(\alpha_1+\gamma)\cdot d_1 - U_2 \cos(\alpha_2+\gamma)\cdot d_2 = 0 \qquad (2.16)$$

where ε is defined

$$\varepsilon = \frac{d_2}{d_1} . \qquad (2.17)$$

vi) Cavity Closure Condition

The new boundary condition to be added is written

$$f_7 \equiv y_c - f_u(x_c) = 0 \qquad (2.18)$$

where

$$x_c = x_b + \frac{1}{\sqrt{1+\sigma}} \int_b^c \cos g_c(\xi') \frac{dW}{d\xi'} d\xi' \qquad (2.19)$$

$$y_c = y_b + \frac{1}{\sqrt{1+\sigma}} \int_b^c \sin g_c(\xi') \frac{dW}{d\xi'} d\xi' \qquad (2.20)$$

f_u = the upper surface shape of the foil.

2.2 NUMERICAL RESULTS WITH THE NEW THEORY

The two computer programs (PCASE and PCASLE) developed above were used to calculate the lift and drag forces for the propeller blade sectional profiles of the Hydronautics 7607.02 propeller. The previous problem of the cavity end-point crossing the blade boundary has, of course, been resolved with these new programs. Figure 2.3 shows the calculated cavity boundary for exactly the same case as that shown in Figure 2.1, proving that the new boundary condition for the cavity end point has properly been implemented in the theory and computer program.

Although the cavity boundary problem was solved, a new type of problem has emerged. Figures 2.4 to 2.9 show the lift, drag coefficients and cavity length as a function of cavitation number over supercavitating and partially cavitating regimes. The force curves of solid lines in these figures are those which had been calculated with the supercavitating (s/c) cascade theory (Furuya 1975), the same as those shown in the previous report (Furuya 1978b), whereas those of broken lines are the newly calculated values with PCASE and PCASLE, covering the partially cavitating regime. It is seen from Figures 2.4 and 2.7 that the lift curves, as they approach a point of $\ell_c/c = 1$ from the two regimes, in some cases match but in other cases do not, depending upon the incidence angle and spanwise location. On the other hand, the drag values calculated from the partially cavitating cascade theory did not agree with those of the s/c cascade theory near $\ell_c/c = 1$ for all cases. Table 2.1 shows most of those data near $\ell_c/c = 1$.

Figures 2.6 and 2.9, which show the relationship between the cavity length and cavitation number, more clearly indicate the mismatching between the two theories. In addition to the mismatching of the data at $\ell_c/c = 1$, we ran into difficulty in understanding the physical meanings of the computed results for smaller incidence angles than $\alpha_1 = 4°$, such as $\alpha_1 = 2°$, $0°$, etc. For those smaller incidence angles, the cavitation number which

was determined in the program decreased as the specified length of cavity was decreased. It must be pointed out that we shall not totally blame the partially cavitating cascade theory for the mismatchings discovered above. When the upper cavity boundaries calculated by the s/c cascade theory were plotted, it was found that they crossed the blade boundaries particularly for small incidence angle cases (see Figures 2.10 and 2.11) at the spanwise locations 50% and 60%, respectively. In Figure 2.10 at $\alpha_1 = 8°$ the calculated cavity boundaries cleared the upper trailing edge of the blade for all σ's whereas at $\alpha_1 = 4°$ the last σ for which the cavity boundary cleared the edge was at .22. It means that the supercavitating cascade data at $\alpha_1 = 4°$ for σ's less than about .22 are physically unacceptable for this blade profile at x = .5. A similar situation also exists in Figure 2.11 for the flow at the spanwise location of 60%.

2.3 APPLICATION OF THE NEW p/c CASCADE DATA TO A CAVITATING PROPELLER

The objective of the present work is to determine the effect of using the data of the partially cavitating cascade flow on the propeller performance prediction method. Previously, even for the regime of the partially cavitating condition, the data of supercavitating cascade theory were used, leading to significant deviation of the predicted performance from the experimental results (see Furuya 1978b).

Although the discrepancies existed between the s/c cascade data and the present p/c cascade data, these partially cavitating cascade data were read from Figures 2.4, 2.5, 2.7, and 2.8 and fed into the propeller program "SCPROP2" of Furuya (1978b) as part of the input data. We know in advance, therefore, that the calculated results from SCPROP2 might not be as accurate as they should be but would indicate the validity of the present concept of incorporating the partially cavitating cascade theory into the cavitating propeller theory.

Calculations were made for two different cavitation numbers, σ_{Va} = .343 and 3.0 for the Hydronautics 7607.02 propeller (σ_{Va} is the cavitation number based on the ship advance speed). The results for the thrust, torque coefficients and efficiency are shown in Figures 2.12 and 2.13, respectively, in comparison with the experimental data of Peck (1977) and Bohn (1977) as well as with the previous theoretical data of Furuya (1978b). For σ_{Va} = .343 which is the design cavitation number, the new calculations provided a slight improvement over the previous prediction, but not significantly. In Figures 2-13(a-d) the detailed information for the local incidence angles, cavitation numbers and lift and drag coefficients is shown as a function of spanwise location x at various J's. It is seen from these data that at J = 0.9 to 1.2, the local flow remains in the supercavitating condition. The effect of using the partially cavi-

tating cascade data in the propeller program is not clearly seen except that the calculations of force coefficients were influenced by the lower values of p/c cascade data during the force interpolation procedure. Furthermore, it should be noted that for the cases of small incidence angles the p/c cascade theory had difficulty in obtaining convergent solutions. Since such data were scarce, "SCPROP2" extrapolated from those of higher incidence angles. This may be one of the reasons for which the performance prediction of the propeller at partially cavitating regime with the present method has not provided significant improvement.

On the other hand, for $\sigma_{Va} = 3.00$, the present method has over-corrected the thrust and torque coefficients for a range of J's in which the partially cavitating condition appears (i.e., $J \geq .55$), see Figure 2.14. From the detailed information in Figure 2.15 a sudden jump in various key quantities such as α_e, C_L, etc., from J = .50 to J = .60 is seen, indicating that "SCPROP2" program used the data of partially cavitating range for J's larger than 0.60. An abrupt change in K_T and K_Q in Figure 2.14 apparently shows use of inappropriate data for the current propeller analysis. As has been mentioned at the beginning of this section, it seems that the data obtained with the modified partially cavitating cascade theory are not accurate enough to be used for the propeller performance prediction at the partially cavitating regime.

It can be readily concluded from the above findings that more accurate data for the partially cavitating cascade flow are necessary. It is for this reason that the double wake flow model has been introduced for the partially cavitating cascade theory and this will be described in the following section.

3. DOUBLE WAKE MODEL FOR p/c CASCADE FLOWS

3.1 THEORY

As has been discussed in the previous section, there has existed the discrepancy in forces and cavitation numbers between the supercavitating cascade theory (Furuya, 1975) and present partially cavitating cascade theory as the cavity length approaches that of the chord. This posed a problem, particularly for foils having blunt trailing edges but not for the sample case shown in Furuya (1978) in which the plano-convex cascade having a sharp trailing edge was used. Figure 3.1 shows two different flow configurations as the cavity length approaches the chord length both from the partially cavitating condition side and supercavitating condition side. The major difference between these two limiting cases lies in the base pressure; it is p_2 for the partially cavitating flow model whereas that is p_c for the supercavitating flow model. These two pressures are quite different, p_c being usually much lower than p_2. This discrepancy will remain in these flow models indefinitely no matter now closely the cavity length is forced to become that of chord. The pressure distributions shown in Figures 3.2(a) and 3.2(b) clearly indicate the above discrepancy; particularly note the differences in the base pressure.

Another aspect to be questioned regarding the flow model currently used in the partially cavitating cascade flow is the single wake flow configuration. In the fully established wake flow around a body having blunt trailing edge, two different types of wake regions are observed experimentally. The first region appears right behind the body and is enclosed by the thin and rather steady free shear layers, which may be called "the near wake". The pressure inside this near wake is nearly constant, designated p_w. Further downstream, the shear layer gradually becomes wider as the vorticity diffuses, generating an irregular flow and then turbulent mixing flow. The flow inside this region is unsteady and stationary only in the mean.

This portion of the wake may be called "the far wake", along which the mean pressure gradually recovers from p_w to p_2 of downstream infinity ($p_2 = p_1$ for the unbounded flow).

In light of the observations on the real wake flow discussed above, a new flow model for the partially cavitating cascade problem is proposed and discussed herein. The idea, which has come out of one of the author's recent discussions with Professor Acosta at the California Institute of Technology, is to represent the real wake flow as closely as possible by using two wakes, behind the body, see Figure 3.3(a). In this flow model, which we call "double wake" model, the pressures p_w in the "near wake" and p_2 in the "far wake" are assumed constant. The problem of this flow model is the method of determining p_w, which is expected to resolve the discrepancy which existed in the previous flow model. Professor Acosta's proposal goes to this point; i.e.,

$$p_w = p_c \cdot \frac{\ell}{c} + p_2 \cdot (1 - \frac{\ell}{c}) \qquad (3.1)$$

It means that the "variable" pressure p_w in the near wake is determined depending upon the cavity length. As the cavity length becomes that of chord, p_w becomes the cavity pressure p_c whereas $p_w = p_2$ is used when the partial cavity totally disappears. The most significant feature of this variable pressure concept is that the smooth blending of the partially cavitating flow into the supercavitating flow may be obtained. Although the validity of linearly interpolating p_w between p_c and p_2 should be proved in comparison with experimental data, Equation (3.1) holds true at least at the limiting case as $\ell \to c$ or $\ell \to 0$. An alternative way of determining the boundary condition on the near wake is to use the velocity instead of the pressure,

$$q_w = U_c \cdot \frac{\ell}{c} + U_2 \ (1 - \frac{\ell}{c}). \qquad (3.2)$$

Using the same potential function and cascade mapping function as before (Furuya, 1978), the physical flow field will be mapped into the potential plane (Figure 3.3(b)) and then into the transform plane ζ (Figure 3.3(c)). The only difference in the ζ-plane from that of Furuya (1978) is that the new ξ-coordinate points g and h have been added, representing the lower and upper near-wake end points, respectively.

The boundary conditions for the present new flow model will be expressed in terms of either the real or imaginary part of ω as follows.

i) <u>On the Far Wake</u>:

$$\tau = 0 \quad , \quad -\infty<\xi<g \text{ and } h<\xi<\infty,$$

ii) <u>On the Near Wake</u>:

$$\tau \equiv \tau_w = \begin{cases} \ln\left\{\frac{\sqrt{1+\sigma}}{U_2}\frac{\ell}{c} + \left(1-\frac{\ell}{c}\right)\right\} & \text{for the Pressure Condition,} \quad (3.3) \\ \ln\left\{1-\left(1-\sigma-\frac{1}{U_2^2}\right)\frac{\ell}{c}\right\}^{\frac{1}{2}} & \text{for the Velocity Condition,} \quad (3.4) \end{cases}$$

$$g<\xi<-1 \text{ and } f<\xi<h,$$

iii) <u>On the Cavity</u>:

$$\tau = \ln\frac{\sqrt{1+\sigma}}{U_2} \quad , \quad b<\xi<c,$$

iv) <u>On the Solid Boundaries</u>:

$$\theta = \begin{cases} \beta_1 & , \quad -1<\xi<0, \\ \beta_1+\pi & , \quad 0<\xi<b, \\ \beta_2+\pi & , \quad c<\xi<f, \end{cases}$$

where the Bernoulli equation has been used for the velocity condition on the near wake. Since there is no change in the branch cuts or singularities, the homogeneous solution $H(\zeta)$ to the problem should remain the same as before (Furuya 1978),

$$H(\zeta) = \sqrt{\frac{(\zeta+1)(\zeta-b)(\zeta-f)}{\zeta-c}} \ .$$

The general solution which satisfies the above mixed-type boundary condition can be readily written by adding two new terms to the solution $\omega(\zeta)$ of Equation (2.5) in Section 2. Defining $\omega_w(\zeta)$ as the general solution to the double wake model flow, one can express it in a form

$$\omega_w(\zeta) = \omega(\zeta) + \sqrt{\frac{(\zeta+1)(\zeta-b)(\zeta-f)}{\zeta-c}} \frac{1}{2\pi i} \left\{ \int_g^{-1} \frac{2i\tau_w}{-\sqrt{\frac{(\xi'+1)(\xi'-b)(\xi'-f)}{\xi'-c}}} \frac{d\xi'}{\xi'-\zeta} \right.$$

$$\left. + \int_f^h \frac{2i\tau_w}{\sqrt{\frac{(\xi'+1)(\xi'-b)(\xi'-f)}{\xi'-c}}} \frac{d\xi'}{\xi'-\zeta} \right\} \qquad (3.5)$$

where $\omega(\zeta)$ is given in Equation (2.5) and

τ_w = Equation (3.3) or (3.4).

In this problem we have a total of 9 unknown quantities, U_2, α_2, $\tilde{A}$, b, c, f, g, h, requiring 9 equations to determine them uniquely;

i) At the upstream infinity,
$\omega(\zeta_1) = \alpha_1 + i \ln \frac{1}{U_2}$ (2 equations)

ii) At the downstream infinity,
$\omega(\infty) = \alpha_2$ (1 equation)

iii) Length of first arc $\equiv S_1$ (1 equation)

iv) End point of the streamline ($\xi = f$) matches the physical trailing edge: (1 equation)

v) Continuity equation (1 equation)

vi) Length of cavity matches the specified length (1 equation)

vii) Cavity end to land on the upper surface of blade (1 equation)

viii) $\Phi_h - \Phi_g = \Gamma$ (1 equation)

Application of these conditions to Equation (3.5) yields the following nine equations, f_{iw}, i = 1, 9 where f_1, $f_2 \cdots$, g_1, g_2 and g_c are those used in Furuya (1978) or found in Section 2. The new equations, f_{iw} are written by simply adding the new terms due to the change for the boundary conditions to these old terms.

i) <u>At Upstream Infinity</u>:

$$\begin{Bmatrix} f_{1w} \\ f_{2w} \end{Bmatrix} \equiv \sqrt{\frac{(\zeta_1+1)(\zeta_1-b)(\zeta_1-f)}{\zeta_1-c}} \frac{\tau_w}{\pi} \left\{ -\int_g^{-1} \frac{1}{\sqrt{\frac{(\xi'+1)(\xi'-b)(\xi'-f)}{\xi'-c}}} \frac{d\xi'}{\xi'-\zeta_1} \right.$$

$$\left. + \int_f^h \frac{1}{\sqrt{\frac{(\xi'+1)(\xi'-b)(\xi'-f)}{\xi'-c}}} \frac{d\xi'}{\xi'-\zeta_1} \right\} + \begin{Bmatrix} f_1 \\ f_2 \end{Bmatrix} = 0 \qquad (3.6)$$

ii) At Downstream Infinity:

$$f_{3w} = \frac{\tau_w}{\pi}\left[\int_g^{-1} \frac{1}{\sqrt{\frac{(\xi'+1)(\xi'-b)(\xi'-f)}{\xi'-c}}}\, d\xi' - \int_f^{h} \frac{1}{\sqrt{\frac{(\xi'+1)(\xi'-b)(\xi'-f)}{\xi'-c}}}\, d\xi'\right]$$

$$+ f_3 = 0 \qquad (3.7)$$

iii) First Arc Length = S_1:

$$f_{4w} = S_1 - s_{1w}(-1) = 0 \qquad (3.8)$$

where

$$s_{1w}(\xi) = \int_\xi^b sg(\xi)\, \frac{e^{-g_{1w}(\xi)}}{U_2}\, \frac{dW}{d\xi}\, d\xi \qquad (3.9)$$

$$g_{1w}(\xi) = \sqrt{\frac{(\xi+1)(b-\xi)(\xi-f)}{\xi-c}}\, \frac{\tau_w}{\pi}\left[-\int_g^{1} \frac{1}{\sqrt{\frac{(\xi'+1)(\xi'-b)(\xi'-f)}{\xi'-c}}}\, \frac{d\xi}{\xi'-\xi}\right.$$

$$\left. + \int_f^{h} \frac{1}{\sqrt{\frac{(\xi'+1)(\xi'-b)(\xi'-f)}{\xi'-c}}}\, \frac{d\xi}{\xi'-\xi}\right] + g_1(\xi) \qquad (3.10)$$

iv) End Point of the Streamline at $\xi = f$ Matching the Trailing Edge of the Blade:

$$f_{5w} = S_2 - s_{2w}(f) = 0 \qquad (3.11)$$

where

$$s_{2w}(\xi) = \int_c^{\xi} \frac{e^{-g_{2w}(\xi)}}{U_2}\, \frac{dW}{d\xi'}\, d\xi' \qquad (3.12)$$

$$g_{2w}(\xi) = \sqrt{\frac{(\xi+1)(b-\xi)(\xi-f)}{\xi-c}}\ \frac{\tau_w}{\pi} \cdot \left[-\int_g^1 \frac{1}{\sqrt{\frac{(\xi'+1)(b-\xi')(\xi'-f)}{\xi'-c}}}\ \frac{d\xi'}{\xi'-\xi} \right.$$

$$\left. + \int_f^h \frac{1}{\sqrt{\frac{(\xi'+1)(b-\xi')(\xi'-f)}{\xi'-c}}}\ \frac{d\xi'}{\xi'-\xi} \right] + g_2(\xi) \qquad (3.13)$$

In order to determine the second arc length S_2, the end point of cavity should be known. The cavity shape is expressed in terms of ξ-coordinate;

$$x - x_B = \frac{1}{\sqrt{1+\sigma}} \int_b^\xi \cos g_{cw}(\xi')\ \frac{dW}{d\xi'}\ d\xi' \qquad (3.14)$$

$$y - y_B = \frac{1}{\sqrt{1+\sigma}} \int_b^\xi \sin g_{cw}(\xi')\ \frac{dW}{d\xi'}\ d\xi' \qquad (3.15)$$

where

$$g_{cw}(\xi) \equiv \sqrt{\frac{(\xi+1)(\xi-b)(f-\xi)}{c-\xi}}\ \frac{\tau_w}{\pi} \left[-\int_g^1 \frac{1}{\sqrt{\frac{(\xi'+1)(\xi'-b)(\xi-f)}{\xi'-c}}}\ \frac{d\xi'}{\xi'-\xi} \right.$$

$$\left. + \int_f^h \frac{1}{\sqrt{\frac{(\xi'+1)(\xi'-b)(\xi'-f)}{\xi'-c}}}\ \frac{d\xi'}{\xi'-\xi} \right] + g_c(\xi). \qquad (3.16)$$

x_B, y_B are the physical coordinates of the blade leading edge. The end point of the cavity (x_c, y_c) is obtained by setting the upper bound of the above integrals (3.14) and (3.15) to be c. Once (x_c, y_c) are determined, the second arc length S_2 is calculated based on the upper body profile.

v) Continuity Equation:

$$f_{6w} \equiv U_1 \cos(\alpha_1+\gamma)\cdot d - U_2 \cos(\alpha_2+\gamma)\cdot d = 0 \qquad (3.17)$$

vi) Length of the Cavity Matching the Specified Length:

$$f_{7w} \equiv x_c - \ell_c = 0 \qquad (3.18)$$

where x_c is calculated by setting ξ to be c in Equation (3.14).

vii) Cavity End to Land on the Upper Surface of Blade:

$$f_{8w} \equiv y_c - f_u(x_c) = 0 \qquad (3.19)$$

where y_c is calculated by setting ξ to be c in Equation (3.15), and $f_u(x_c)$ is the y-position of upper surface of the blade at x_c.

viii) $\Phi_h - \Phi_g = \Gamma$

$$f_{9w} \equiv \frac{d}{2\pi}\left\{ e^{-i\delta} \ln\left(\frac{\xi_1-h}{\bar{\xi}_1-g}\right) + e^{i\delta} \ln\left(\frac{\bar{\xi}_1-h}{\xi_1-g}\right)\right\}$$

$$- d\left\{\sin(\alpha_1+\gamma) - U_2 \sin(\alpha_2+\gamma)\right\} = 0 \qquad (3.20)$$

Equations (3.6), (3.7), (3.8), (3.9), (3.11), (3.17), (3.18), (3.19) and (3.20) now provide nine independent relationships for nine unknown parameters.

The same numerical method as before (Furuya 1978) will be applied to the above nine functional nonlinear equations for determining the nine solution parameters.

3.2 NUMERICAL RESULTS

A substantial effort has been taken for modifying the previous computer program (PCASLE) in order to implement the theory described above. The new computer program designated "PCASLW" has the nine unknown parameters for the nine independent relationships. The convergence of Newton's iterative method was very slow, costing about $50 of Lawrence Berkeley Laboratory's computer time to obtain results for one data point. Due to the time and budgetary restraints, only a few representative computations were made with the new computer code PCASLW.

Figures 3.4 and 3.5 show the lift and drag coefficients with $\alpha_1 = 4°$ for the blade sectional profile of Hydronautics 7607.02 propeller at x = .5, in comparison with those of the previous computer program (PCASLE). The relationship between the length of cavity and cavitation number for the same case is shown in Figure 3.6. It is seen from these figures that the new theory has provided a significant improvement for both force coefficients and cavity length-cavitation number relationships. A smooth connection between the partially cavitating regime and supercavitating regime was provided by following the result of the new p/c cascade theory up to $\sigma = .22$, for this case, and then going into the supercavitating range. In doing this the data for σ larger than .22, calculated with the s/c cascade theory, should be discarded for the previously mentioned reason (see Section 2.2).

However, the present PCASLW experienced difficulty in obtaining the convergent solution for the case of $\alpha_1 = 8°$ at which the cavity boundaries cleared the blade trailing edge for all σ's at the s/c range and thus a rather smooth matching was obtained with the previous p/c cascade theory (see Figures 2.4 to 2.6). The same difficulty existed for the blade sectional profile at the spanwise location of 60% of Hydronautics 7607.02 at $\alpha_1 = 4°$. It might be coincidental to

observe that for these cases the cavity boundaries clear the blade trailing edge for all σ's in the supercavitating range and the discrepancy for C_L and C_D at $\ell_c/c = 1$ is minor (see Figures 2.7 to 2.9).

For the case of $\alpha_1 = 2°$ at x = .6, although convergent solutions were obtained with the new method, the calculated data showed a peculiar behavior similar to that occurring in $\alpha_1 = 2°$ at x = .5; the calculated cavitation number decreased as the length of cavity decreased. This type of behavior in cavity length vs. cavitation number is anomalous in the cavity flow unless this theoretical finding is interpreted as an indication for unsteady flow phenomena. As a matter of fact, Figure 2.11 indicated that the upper cavity boundary even for a relatively long cavity, i.e., $\ell_c/c = 1.4$ chords, barely cleared the upper blade surface. It is thus questionable if the partial cavity can exist at such a small incidence angle $\alpha_1 = 2°$.

It must also be mentioned that this type of reversal relationship for the cavity length to cavitation number took place for the partially cavitating cascade flow around the plano-convex blade (see Furuya 1978).

4. SUMMARY AND RECOMMENDATION

The objective of the present research work is to incorporate the partially cavitating cascade data into the performance prediction method for cavitating propellers and to determine if any improvement will be made on the previously obtained results (Furuya 1978b). The partially cavitating cascade theory was developed in the first phase of the work, the computer codes developed then being called PCAS and PCASL (Furuya 1978). It was found that this theory can be used only for cascade blades having small camber such as flat or plano-convex blades. For practical blade profiles having rather high camber such as those used for supercavitating propellers, it was discovered that the calculated upper cavity boundary crossed the blade surface, which is physically unacceptable. In order to correct this deficiency, an additional boundary condition that the upper cavity end point be placed on the blade surface was imposed on the previous theory but by allowing the wake to open at downstream infinity. The computer codes developed based on this flow model were designated as PCASE and PCASLE. Although the problem of the upper cavity boundary crossing the blade surface was resolved, a new problem of mismatching, as the length of cavity approaches that of chord, has emerged. It was considered that one of the main reasons for mismatching was attributable to the difference in the base pressure between the partially cavitating and supercavitating cascade theories, leading to the development of another new theory. The new flow model used here was designated as "double wake" flow model in which the near wake was formed immediately after the blunt trailing edge and followed by the far wake. The near wake pressure p_w was determined by a linear interpolation between the cavity pressure p_c and far wake pressure p_2 as a function of the cavity length. By using this interpolation method it was ensured that the base pressure approaches to the cavity pressure as the length of

cavity becomes that of chord. The new computer program, now the third one, called "PCASLW" was applied to the same blade sectional profiles of Hydronautics 7607.02 propeller. For a certain combination of the flow configuration, the calculated data smoothly connected with those of the supercavitating regime as a function of cavitation number. It was found, however, that the program "PCASLW" had difficulty in convergence for large incidence angle cases. This was not surprising because for such cases a sudden jump of the cavity closure point in the y-direction existed between the supercavitating and partially cavitating flows.

Another problem with "PCASLW" was that the relationship between the cavity length and cavitation number was reversed to that usually found in the cavity flow, i.e., the calculated cavitation number decreased as the specified cavity length decreased. This may be interpreted as an indication for a possible unsteady flow phenomenon or for nonexistence of partially cavitating flows for such small incidence angles.

The lift and drag forces calculated based on PCASE and PCASLE programs were incorporated into the propeller program "SCPROP2" for prediction of the high speed propeller performance operating at the partially cavitating regime. Although the data were known to be somewhat inaccurate, the intention of the study was to seek a possibility for improving the prediction capability of the SCPROP2 program for the p/c regime. In fact, the results of computations revealed such an improvement despite the inaccurate data employed.

The following conclusions and recommendations based on the findings from the current study will be thus given.

i) The partially cavitating cascade flow is much more complex than its counterpart, i.e., supercavitating cascade

flow, due to the fact that the upper surface of the blade comes into a part of the boundary conditions. Three different theories and their computer programs have been developed to date under the GHR project, but no single theory can completely cover various flow configurations and cascade geometries. Selection of an appropriate one among these three methods requires careful examination of not only the flow configuration to be solved but also that of the supercavitating condition. No general selection guideline exists except for the fact that the single wake model (PCASE and PCASLE) provided better results in convergence as well as the calculated data for the cases in which the cavity boundary calculated from the s/c theory clears the upper trailing edge near $\ell_c/c = 1$. For the cases in which the cavity boundary crosses the upper trailing edge near $\ell_c/c = 1$, the double wake model (PCASLW) was superior.

ii) Because of the imperfect state of the three partially cavitating cascade theories developed here, it is recommended that a more general theory should be developed with a different set of boundary conditions.

iii) In order to develop a better flow model, more detailed information is necessary from experiments. This should include the relationship between the cavity length and cavitation number, forces, base pressure and stability of the cavity flow for various flow and blade configurations.

iv) The accuracy of the three theories developed here should be determined only in comparison with experimental data.

v) Based on the trial test conducted during this phase of work, it was indicative that more accurate partially cavitating cascade data, if available and used in the high speed propeller theory, will improve the prediction accuracy for cavitating propeller performance. It is, however, too early at this stage to determine which flow model or theory should be used for this purpose. Again we should await the results of experiments, which will clarify many uncertainties mentioned above.

5. REFERENCES

Bohn, J.C., 1977, Model Tests of a Supercavitating Propeller Designed for a Hydrofoil Ship. *Hydronautics Reports, 7607.59, August.*

Furuya, O., 1975, Exact Supercavitating Cascade Theory. *Journal of Fluid Engineering, ASME. Vol. 97, December, 419-429.*

Furuya, O., 1976, Development of an Off-Design Predictive Method for Supercavitating Propeller Performance. *Tetra Tech Report TC-676.*

Furuya, O., 1978, Nonlinear Theory for Partially Cavitating Cascade Flows. *Tetra Tech Report TC 3951-01, also to be presented at the 10th Symposium of IAHR to be held in Japan, 1980.*

Furuya, O., 1978b, Part I: Calculations of the Off-Design Performance for Hydronautics' SC Propeller, Part II: Theory Improvement for Computer Code "SCSCREW". *Tetra Tech Report TC 3913 and 3239.*

Peck, J.G., 1977, Cavitation Performance Characteristics of Supercavitating Propellers 4698 and 4999. *DWTNSRDC Ship Performance Department, Department Report SPD-680-02, December.*

Wade, R.B. and Acosta, A.J., 1967, Investigation of Cavitating Cascade. *ASME, Journal of Basic Engineering, December, 693-706.*

Wu, Y., 1968, Basic Developments in Fluid Dynamics, Vol. 2, Section of Inviscid Cavity Flows. *Academic Press, 22.*

Yim, B. and Higgins, L., 1975, A Nonlinear Design Theory for Supercavitating Cascades. *Proceedings of the Symposium on Cavity Flows, the Fluid Engineering Conference of ASME, held at Minneapolis, Minnesota May 5-7, p. 85-94.*

TABLE 2.1

Lift and Drag Data Near $\ell_c = 1$ Calculated from the Supercavitating (s/c) Cascade Theory and Partially Cavitating (p/c) Cascade Theory

i) At spanwise location x = 0.5 of Hydronautics 7609.02 Propeller

	Item \ Theory	s/c Cascade Theory (1975)	p/c Cascade Theory (Present)
$\alpha_1=8°$	Cavitation Number σ	.450	.495
	Cavity Length ℓ/c	1.020	.900
	C_L	.866	.871
	C_D	.181	.138
$\alpha_1=4°$	σ	.220	.201
	ℓ/c	1.091	.950
	C_L	.405	.369
	C_D	.0546	.0300

TABLE 2.1 (Con't.)

ii) At x = .6

Item \ Theory		s/c Cascade Theory	p/c Cascade Theory
$\alpha_1 = 4°$	σ	.200	.284
	ℓ/c	1.190	.900
	C_L	.398	.505
	C_D	.0954	.0421
$\alpha_1 = 2°$	σ	.115	.102
	ℓ/c	1.400	.900
	C_L	.261	.231
	C_D	.0246	.0126

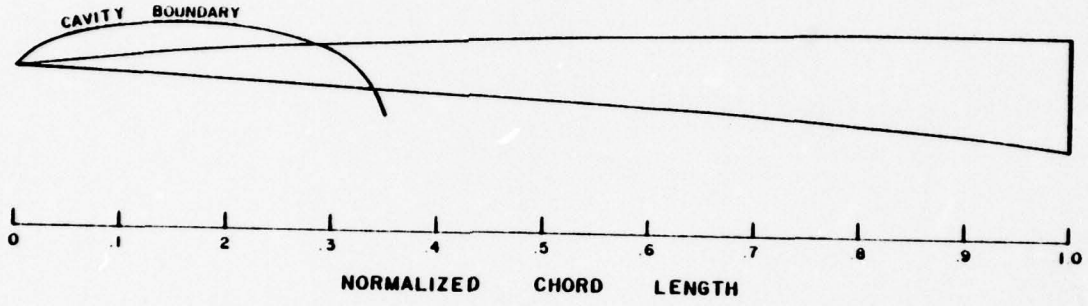

Figure 2.1 Cavity Boundary Calculated with the Previous P/C Cascade Theory (Furuya 1978) for Hydronautics 7607.02 Propeller Blade Section at 50% Span Position, $\alpha_1 = 4°$ and $\ell_c = .35$

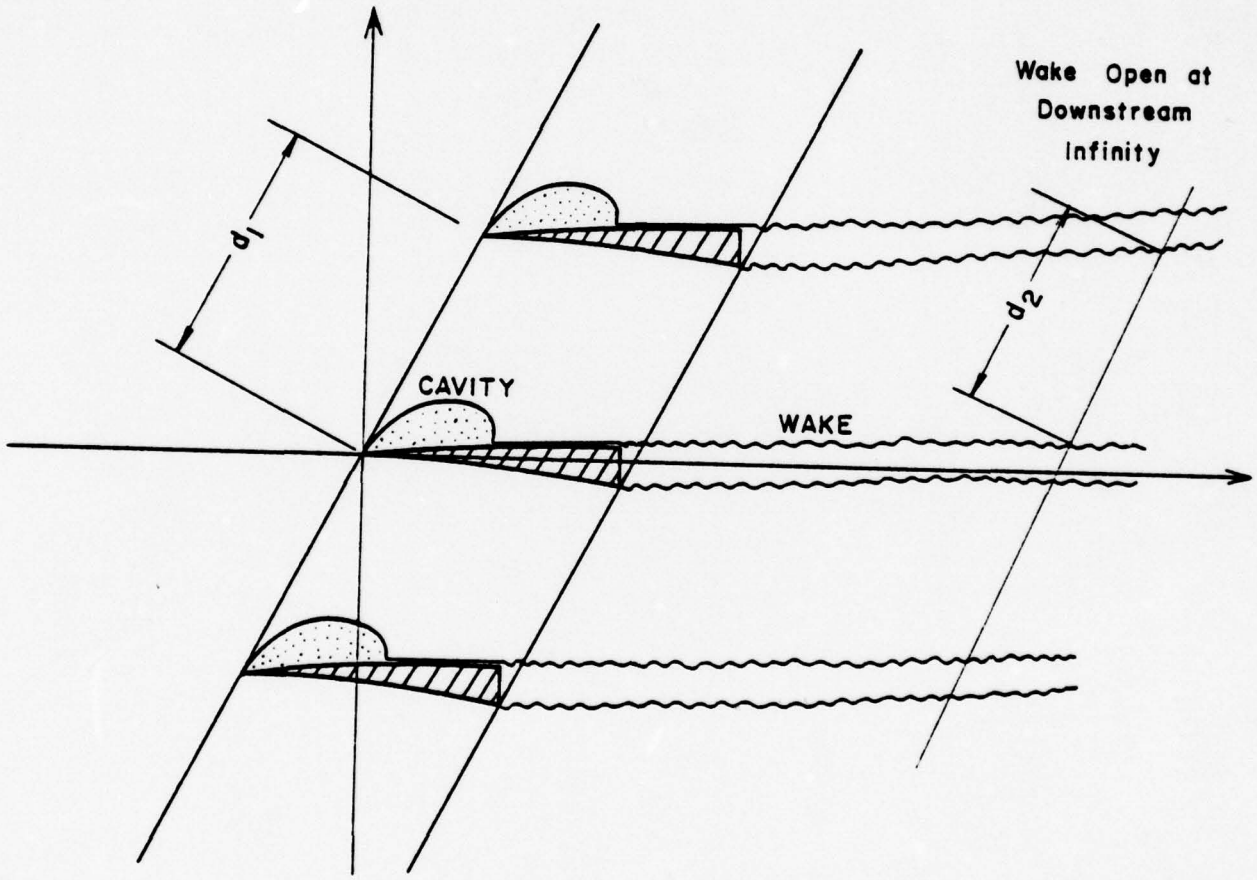

Figure 2.2 Schematic Diagram for the New P/C Cascade Flow Model

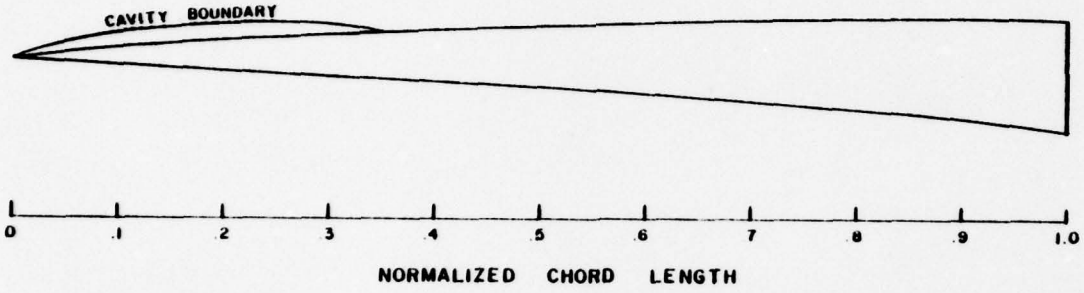

Figure 2.3 Cavity Boundary Calculated with the New Flow Model for the Same Blade as that in Figure 2.1

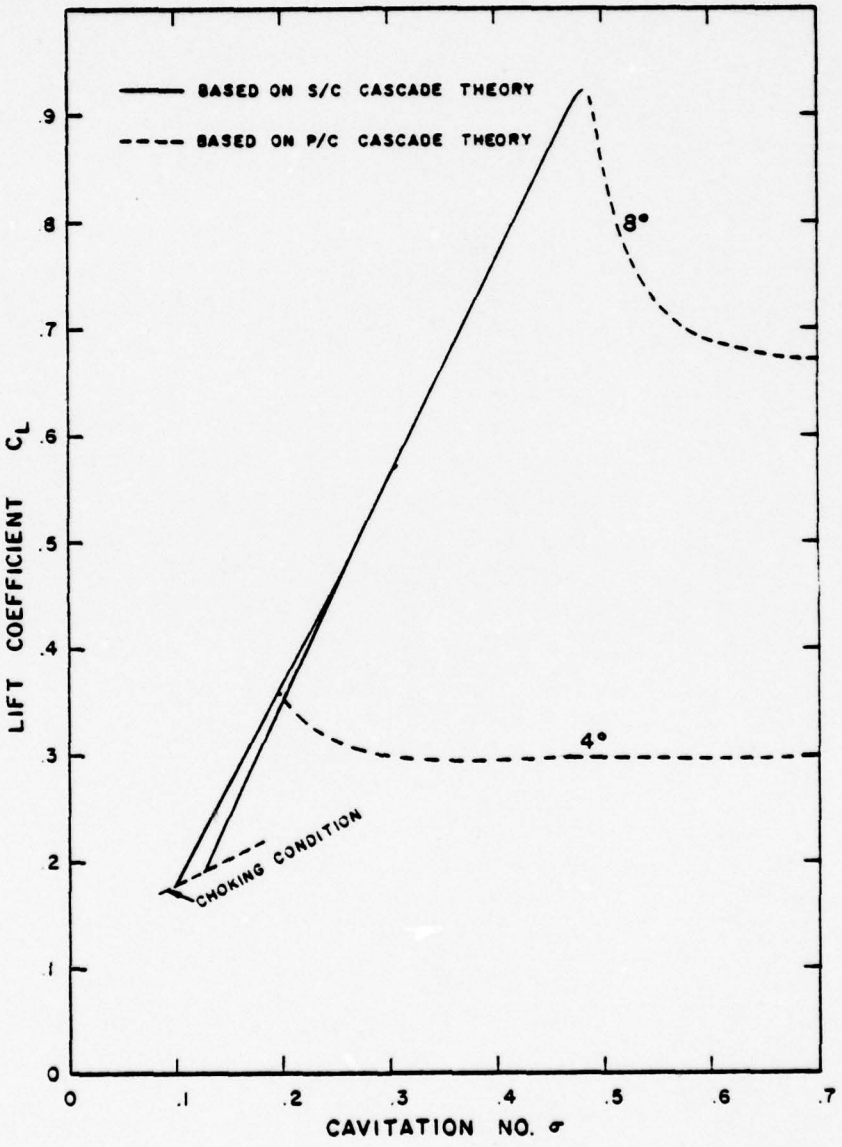

Figure 2.4 C_L vs. σ at x = .5 of Hydronautics 7607.02 Propeller, the C_L Values being calculated with the New Flow Model

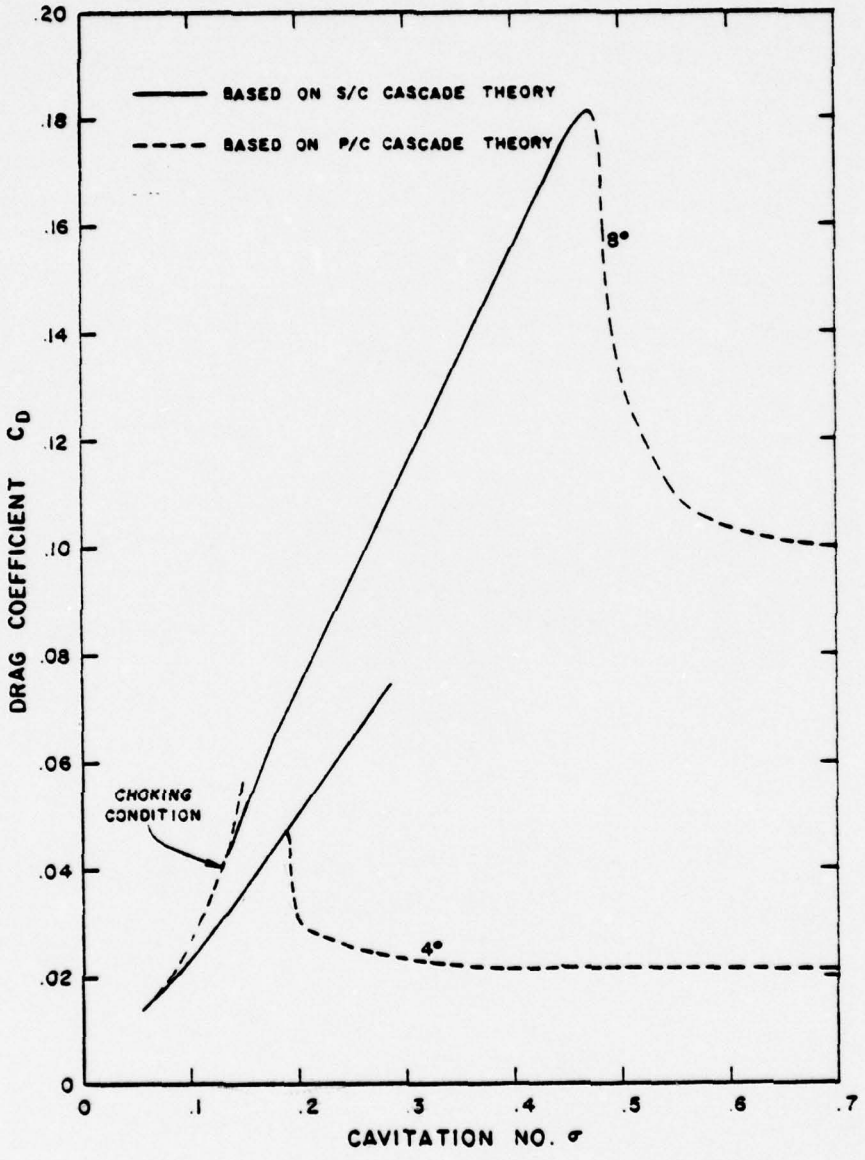

Figure 2.5 C_D vs. σ for the Same Blade as that in Figure 2.4

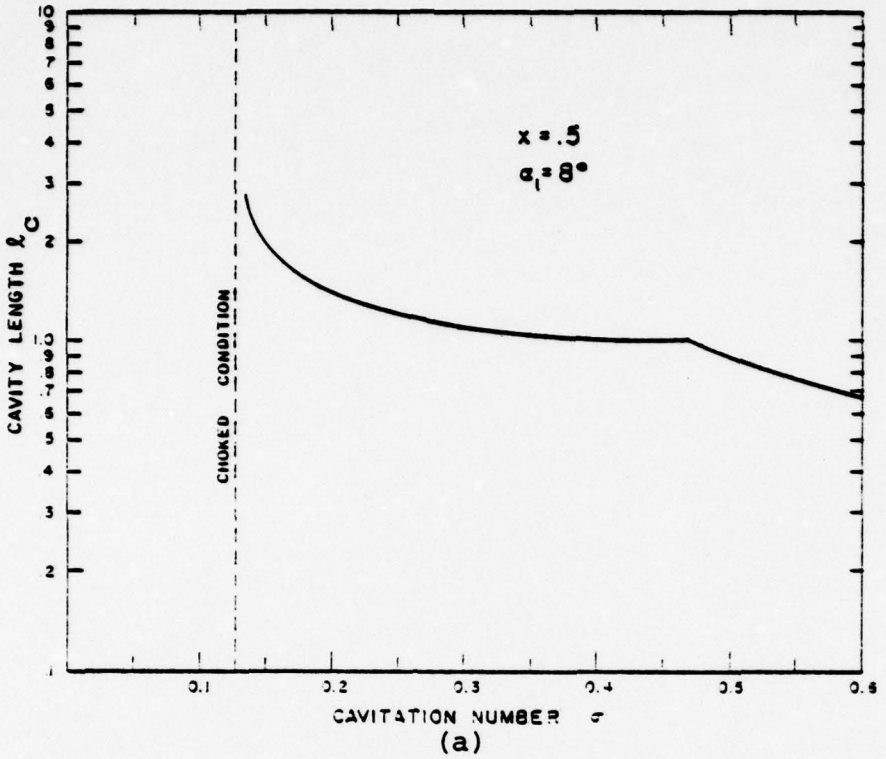

(a)

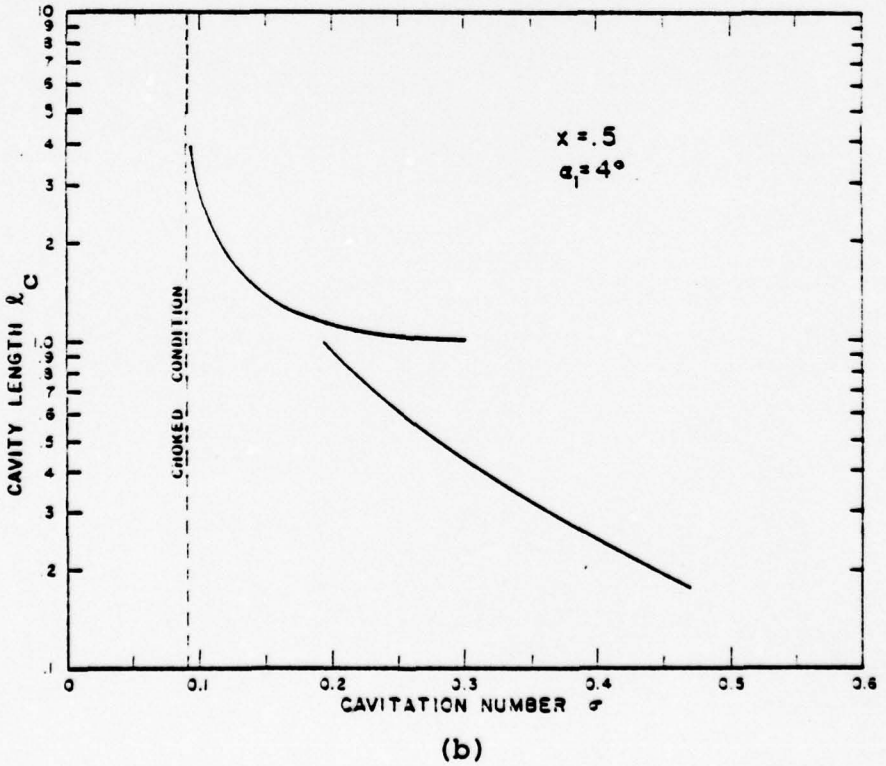

(b)

Figure 2.6 Cavity Length ℓ_c vs. Cavitation Number σ for the Cases of Figure 2.4 and 2.5

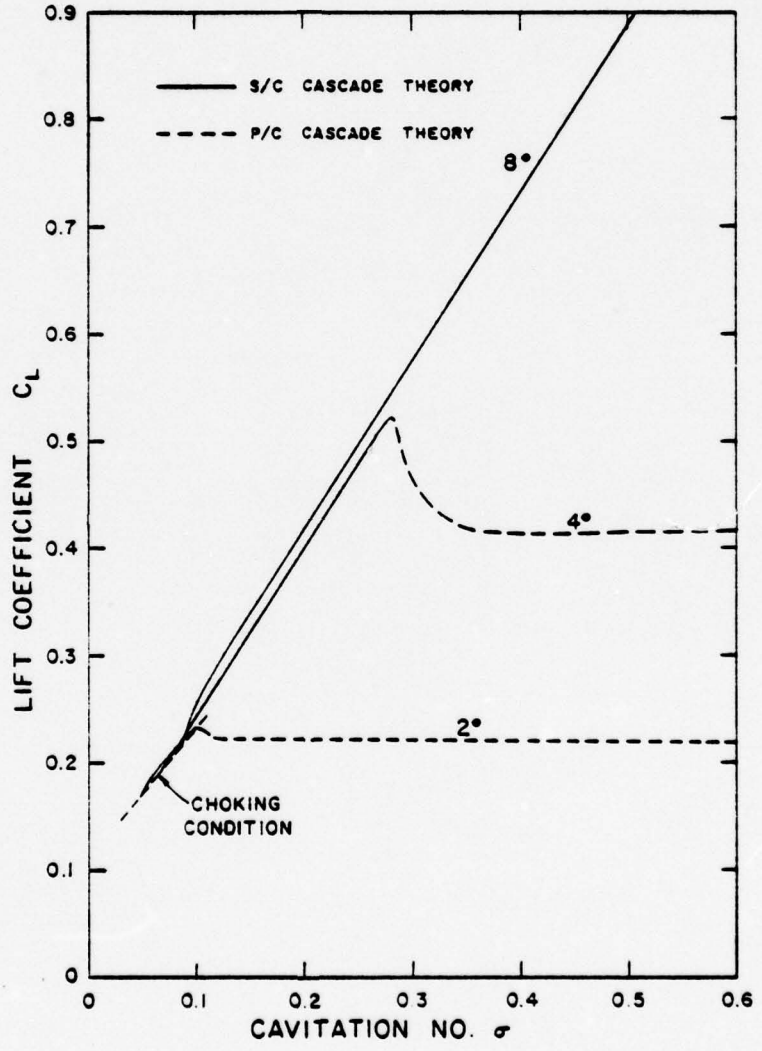

Figure 2.7 C_L vs. σ at x = .6 of Hydronautics 7607.02 Propeller, the C_L values being calculated with the New Flow Model

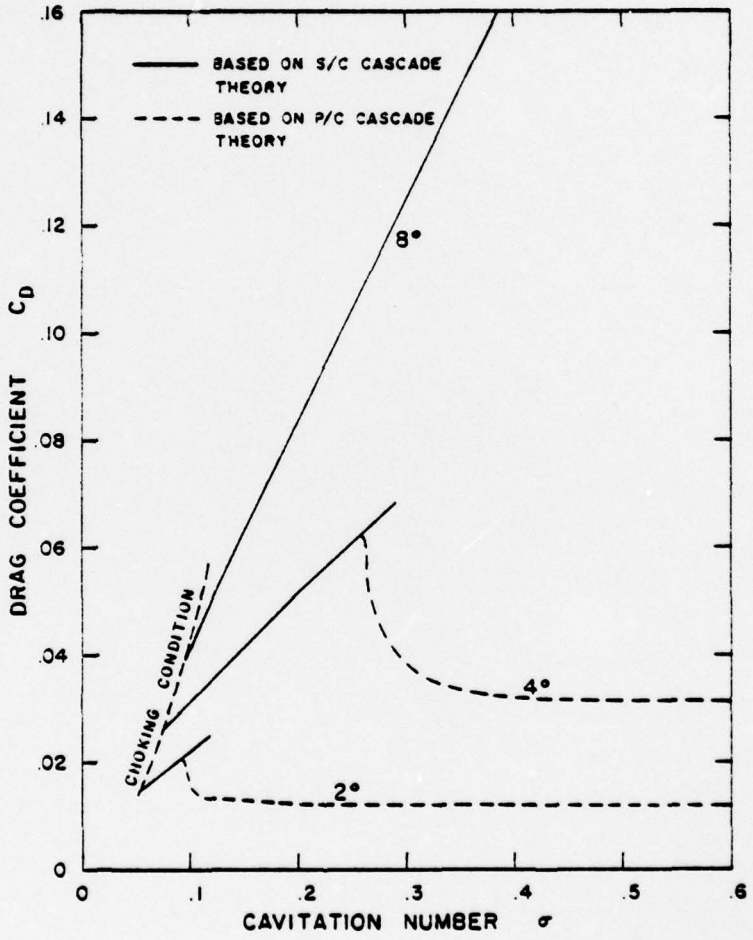

Figure 2.8 C_D vs. σ for the Same Blade Section as that of Figure 2.7

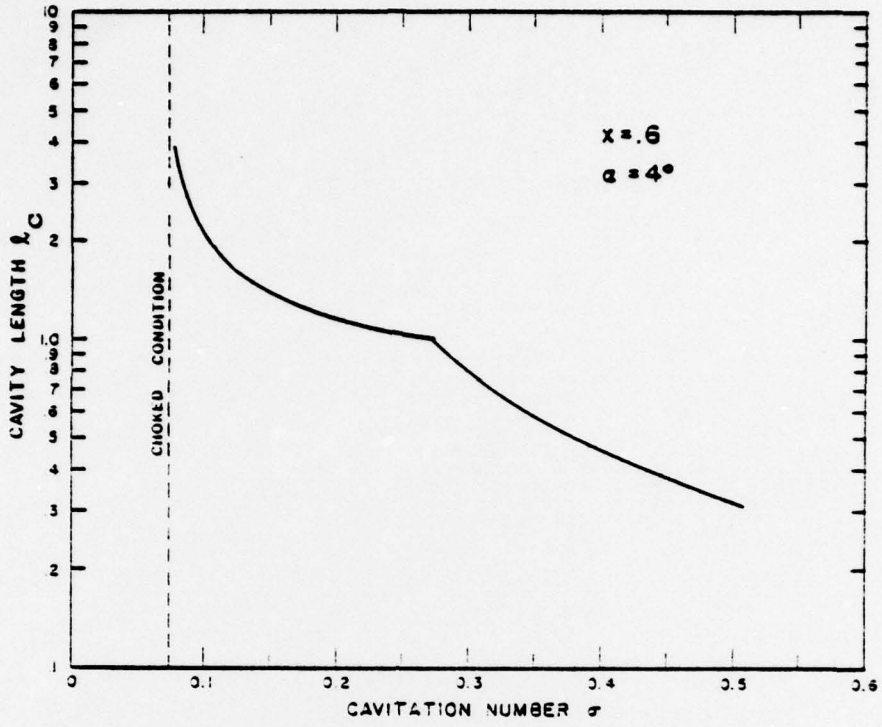

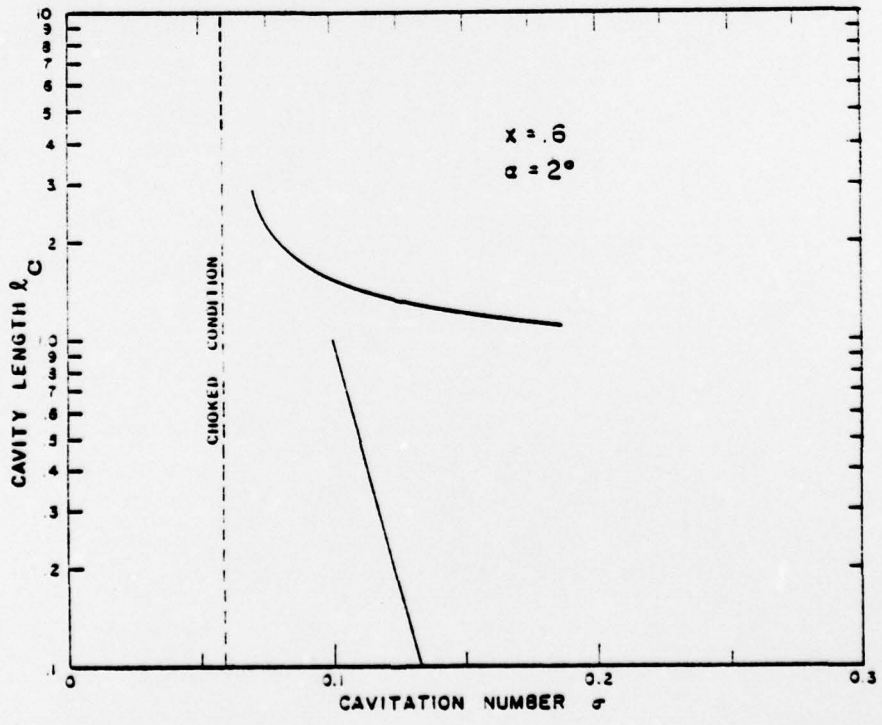

Figure 2.9 Cavity Length ℓ_c vs. Cavitation Number σ for the Cases of Figures 2.7 and 2.8

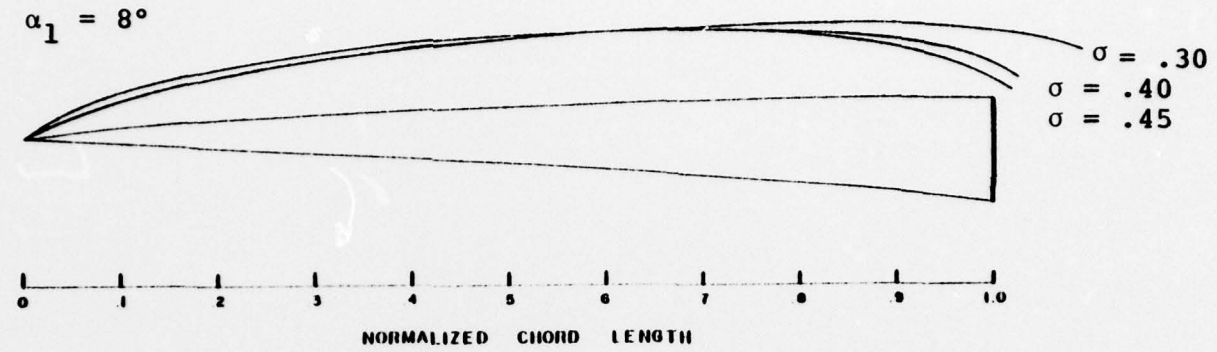

Figure 2.10 Locations of the Calculated Cavity Boundaries for the Blade Profile at the Spanwise Position of 50% of Hydronautics 7607.02

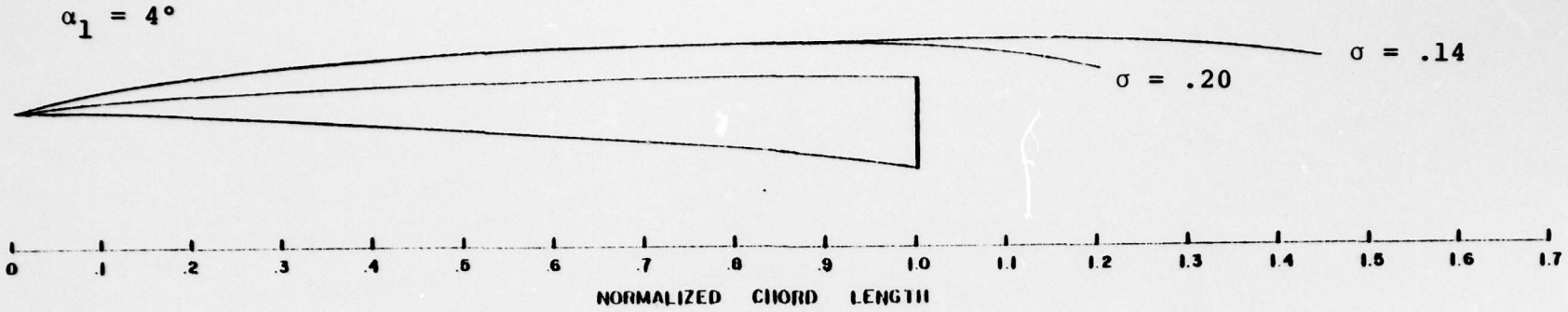

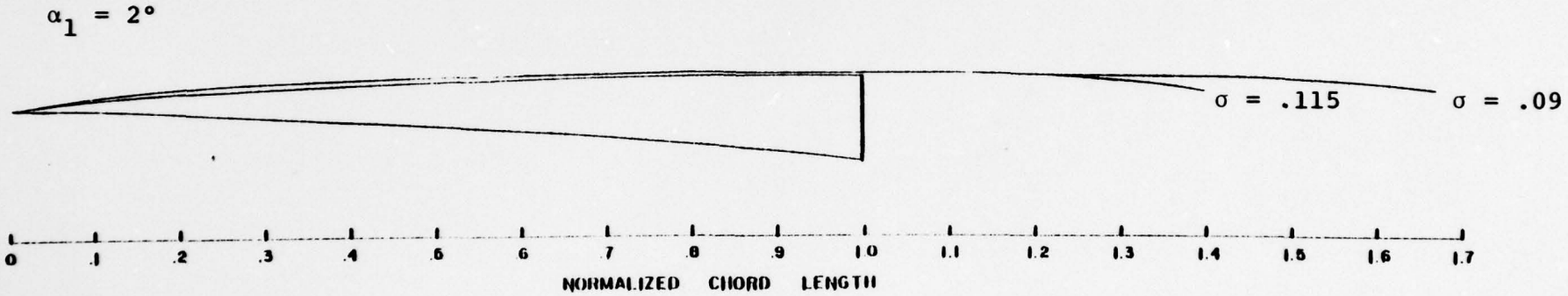

Figure 2.11 The Same as that of Figure 2.10 except that the Spanwise Location is 60%

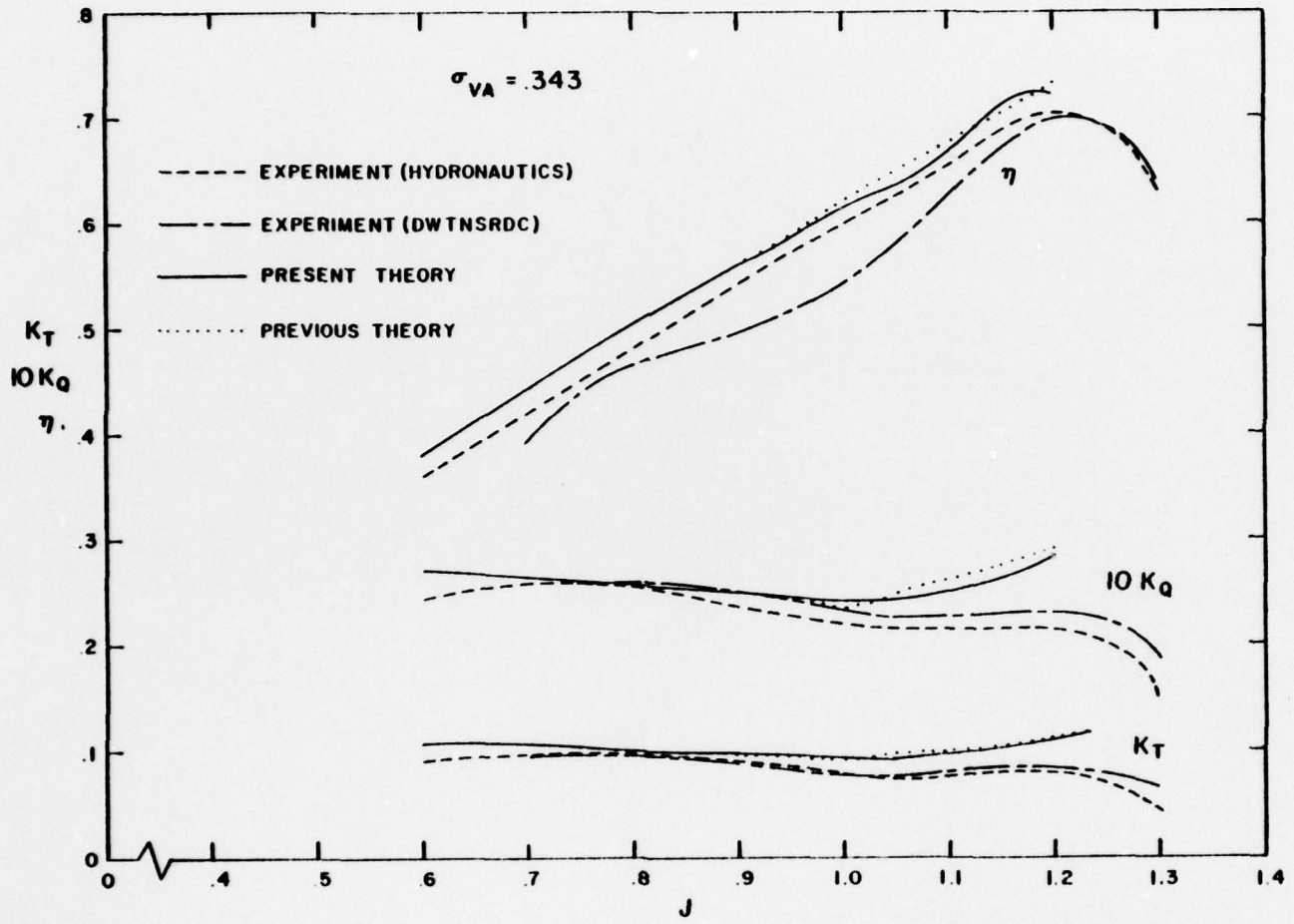

Figure 2.12 Comparison of the Present Results for K_T, K_Q and η of Hydronautics 7607.02 at σ_{Va} = .343 with those of the Previous Theory (Furuya 1978b) and Experiments (Bohn 1977 and Peck 1977)

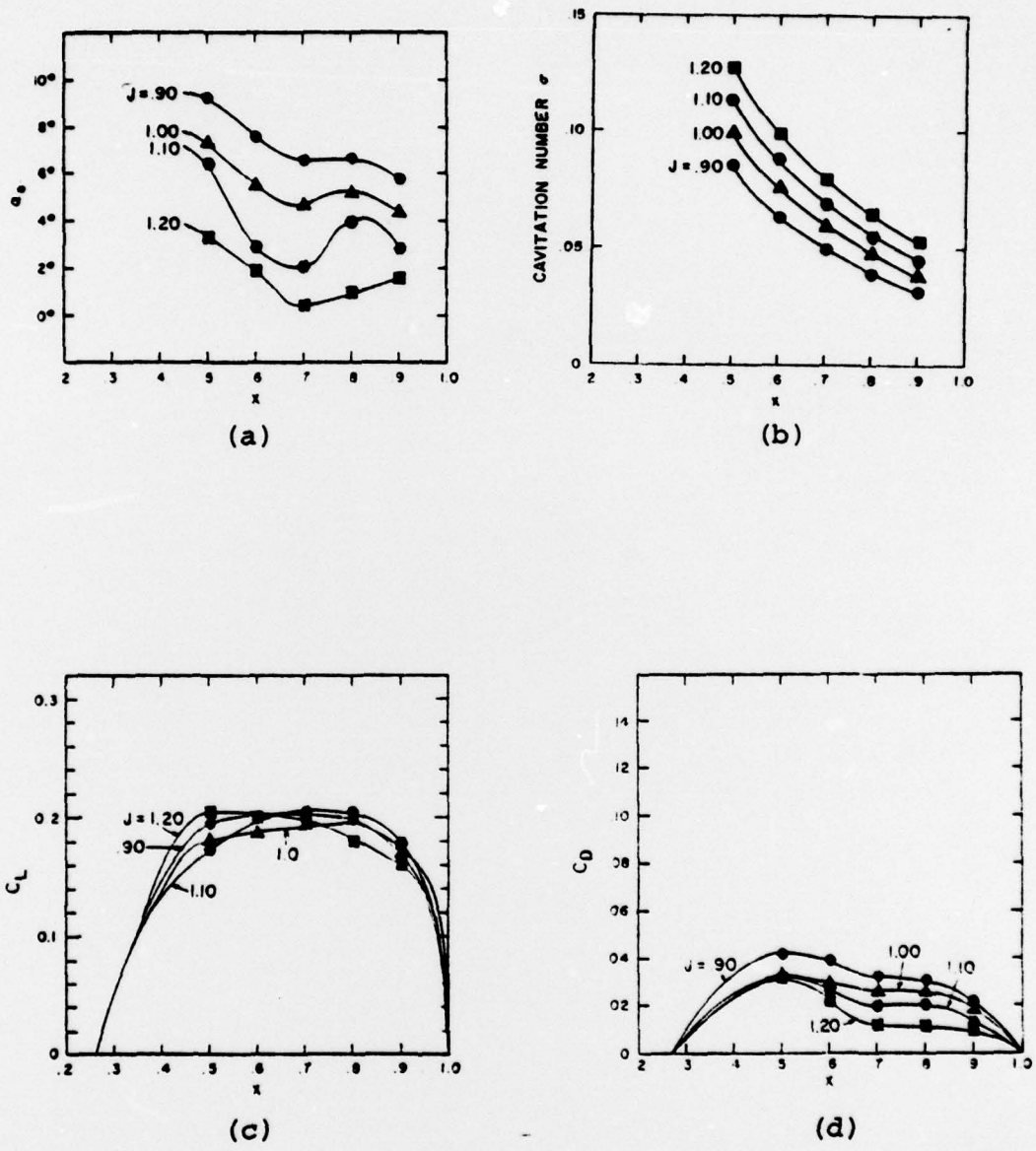

Figure 2.13 Propeller Sectional Data for Figure 2.10 Where x Designates the Normalized Spanwise Location

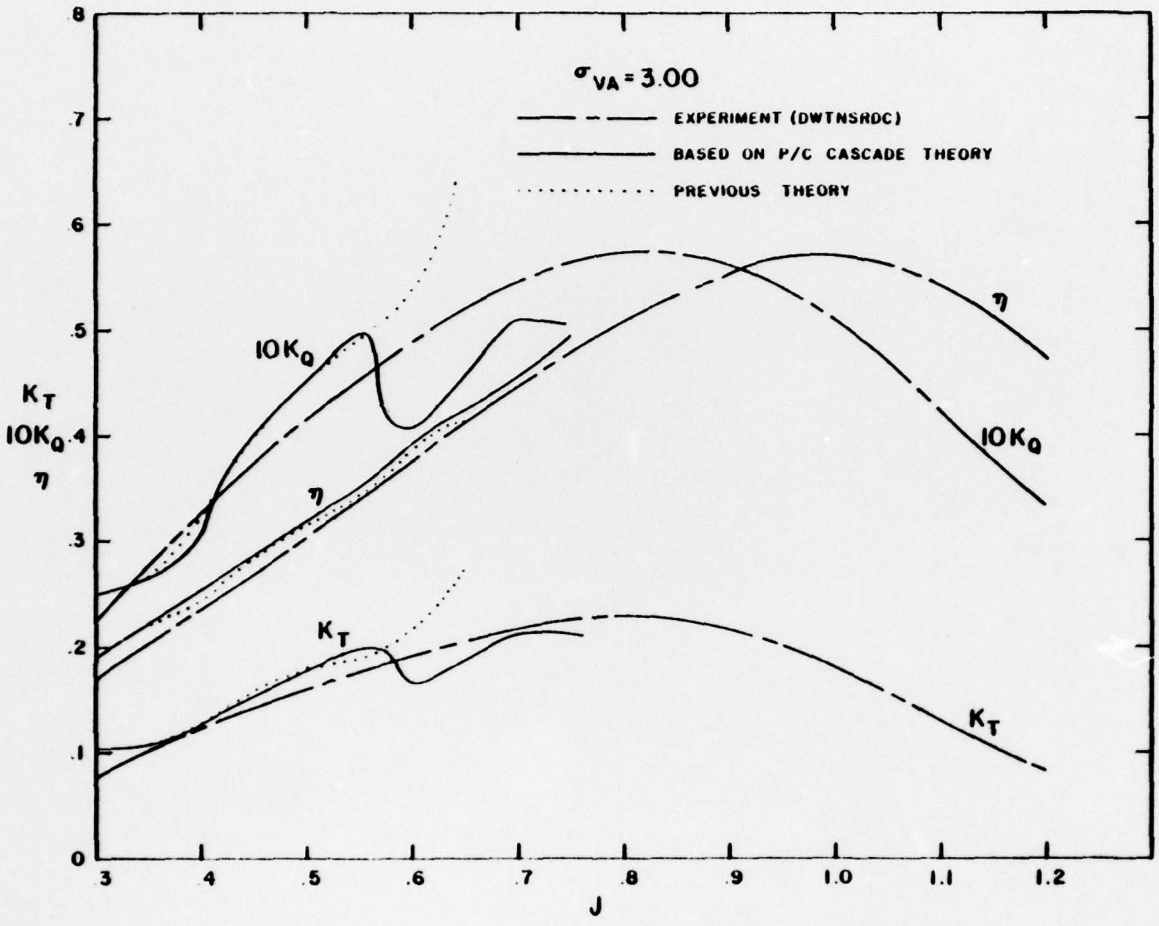

Figure 2.14 The Same as Figure 2.10 except that this is the case for σ_{Va} = 3.0

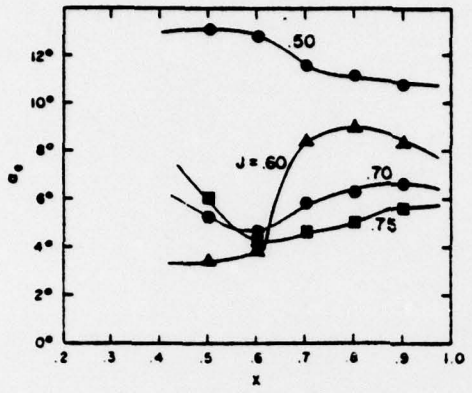

(a)

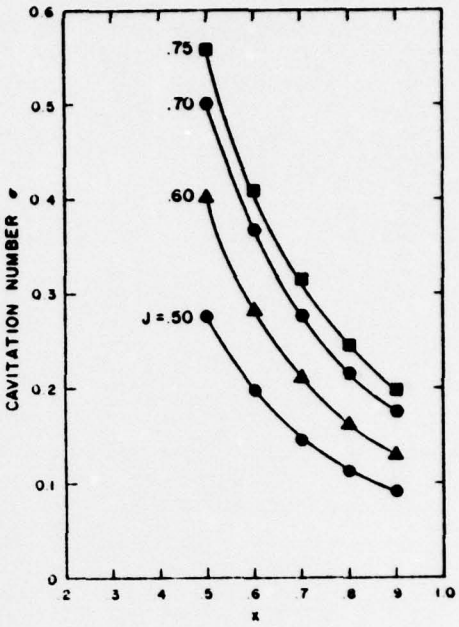

(b)

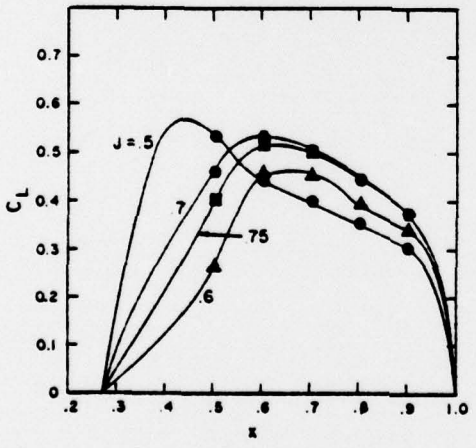

(c)

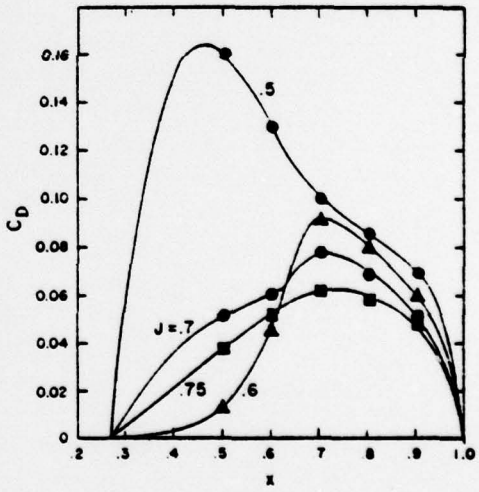

(d)

Figure 2.15 Propeller Sectional Data for Figure 2.12

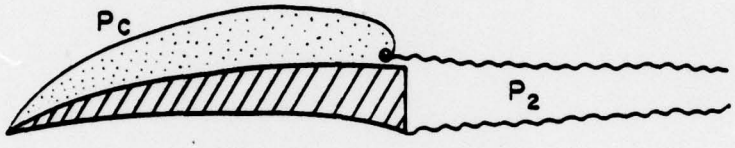

(a) Partially Cavitating Condition

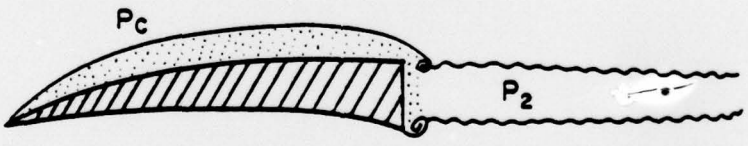

(b) Supercavitating Condition

Figure 3.1 Comparison of the Flow Configuration Between the Partially Cavitating Condition and Supercavitating Condition as the Cavity Length approaches to the Chord Length

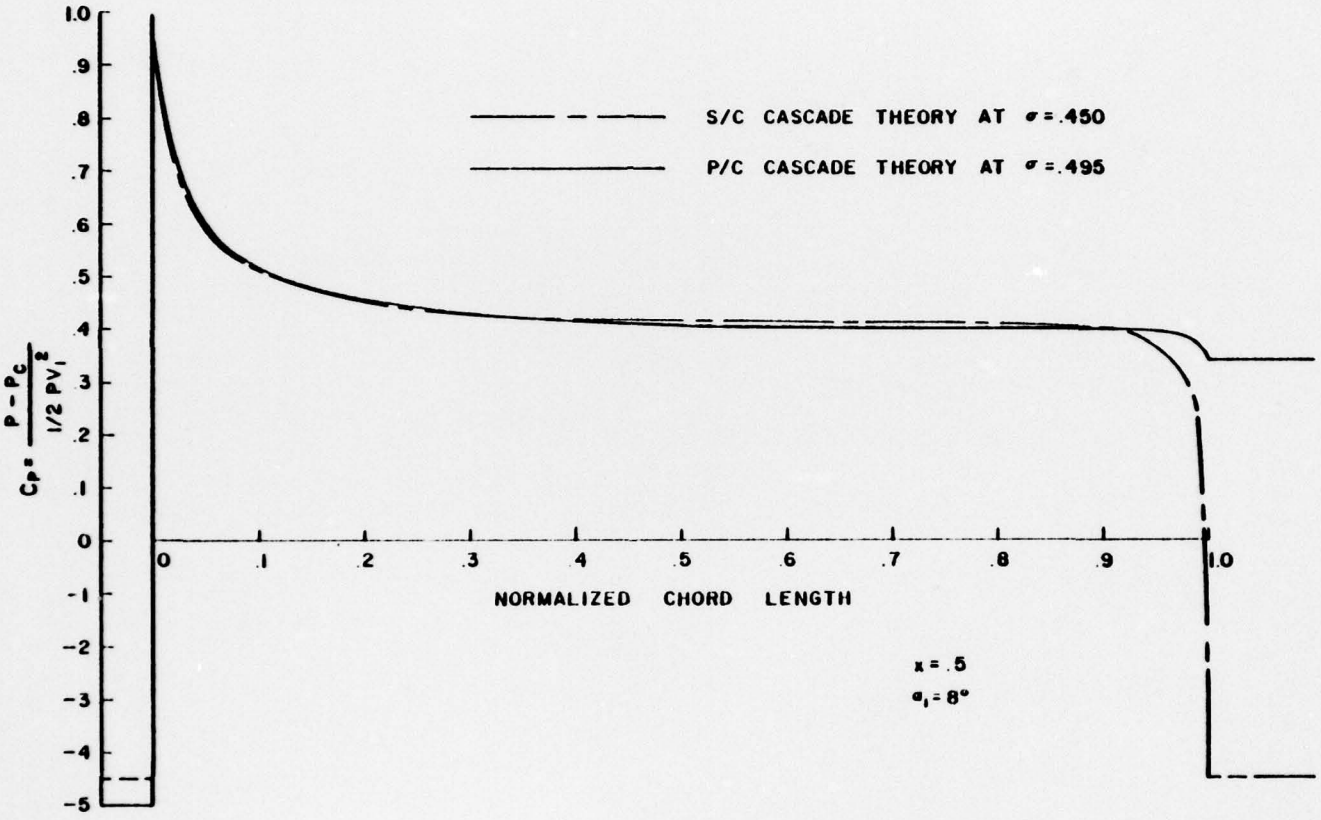

Figure 3.2(a) Comparison of the Pressure Distribution of the Pressure Side Between the P/C Cascade Theory (Furuya 1978) and S/C Cascade Theory (Furuya 1975) for the Hydronautics Propeller 7607.02 Section at x = .5 and α_1 = 8°

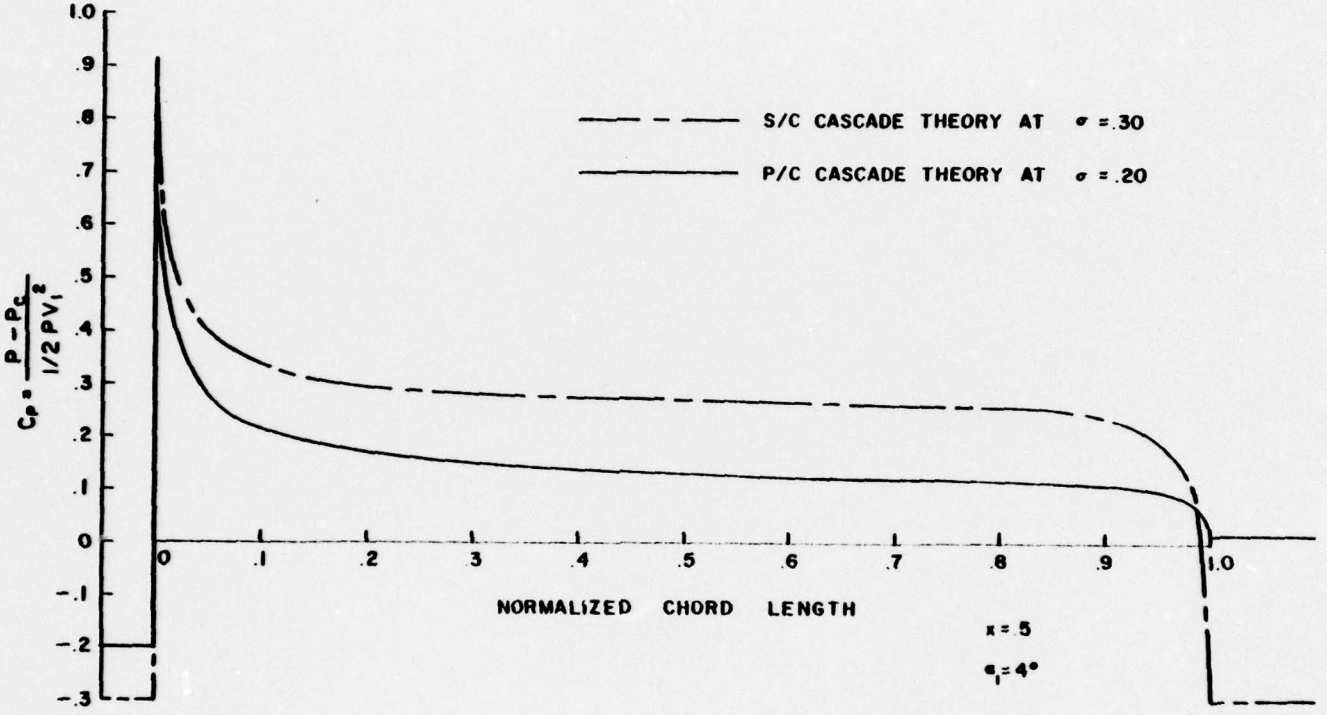

Figure 3.2(b) The Same as Figure 3.2(a) except that these are the cases for $\alpha_1 = 4°$

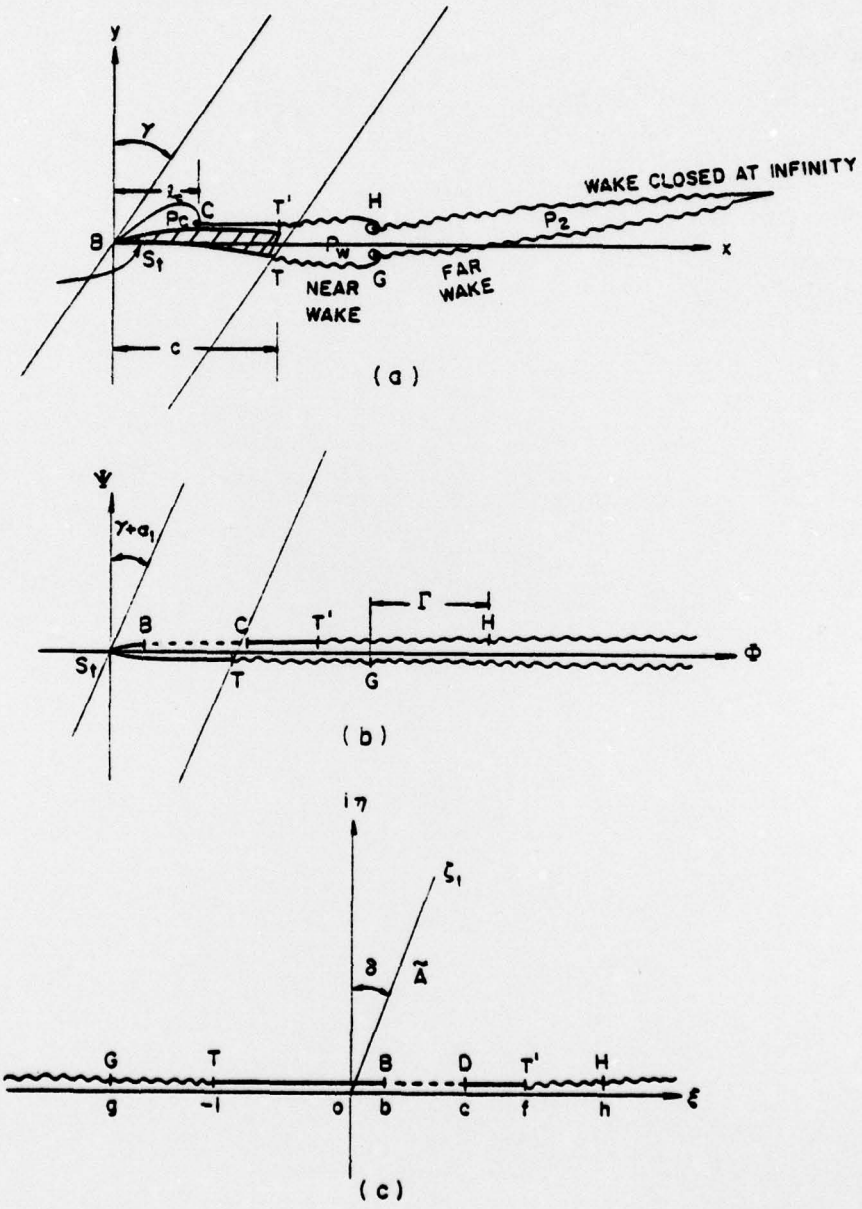

Figure 3.3 Schematic Diagram for the Double Wake Model for the Partially Cavitating Cascade Flow and its Mapping Planes

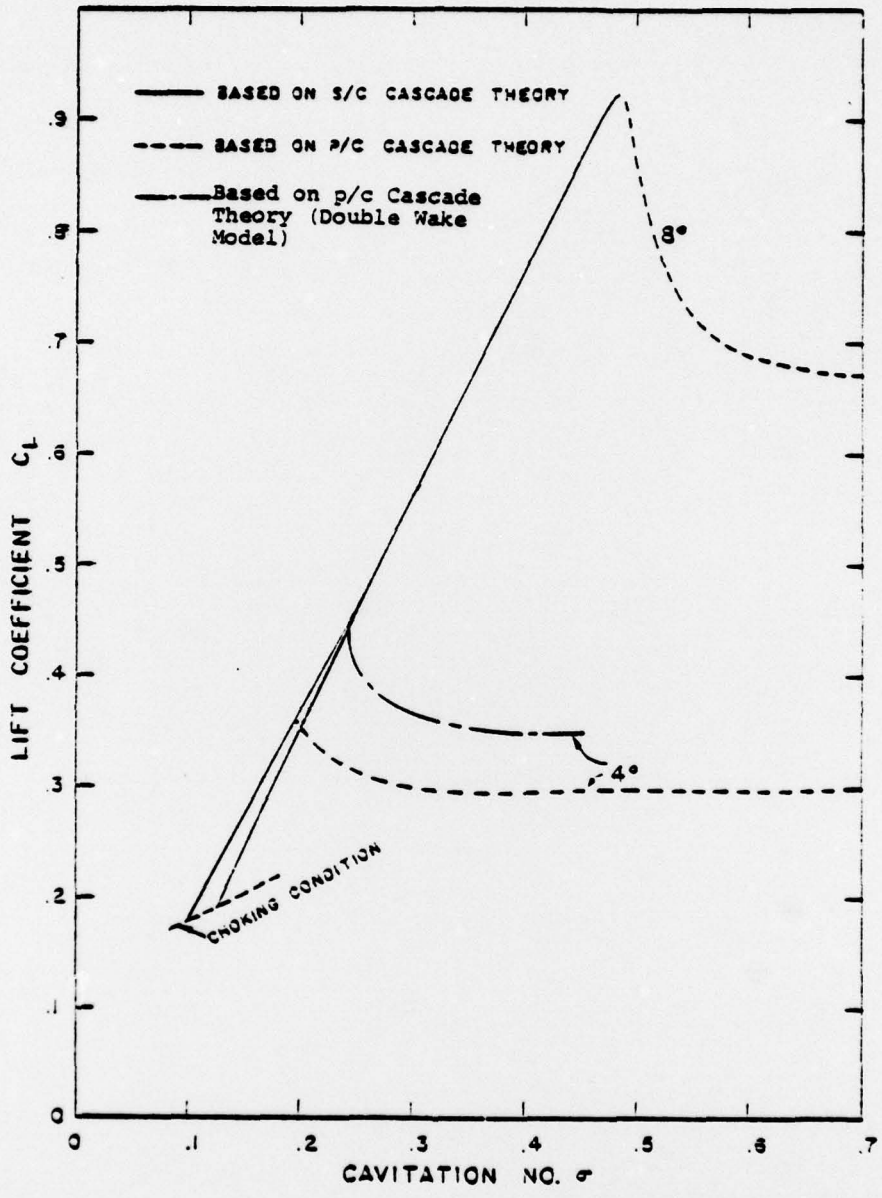

Figure 3.4 Lift Coefficient vs. Cavitation Number Calculated with the New Partially Cavitating Cascade Theory in Comparison with the Previous Theory at x = 0.5 for Hydronautics Propeller 7607.02

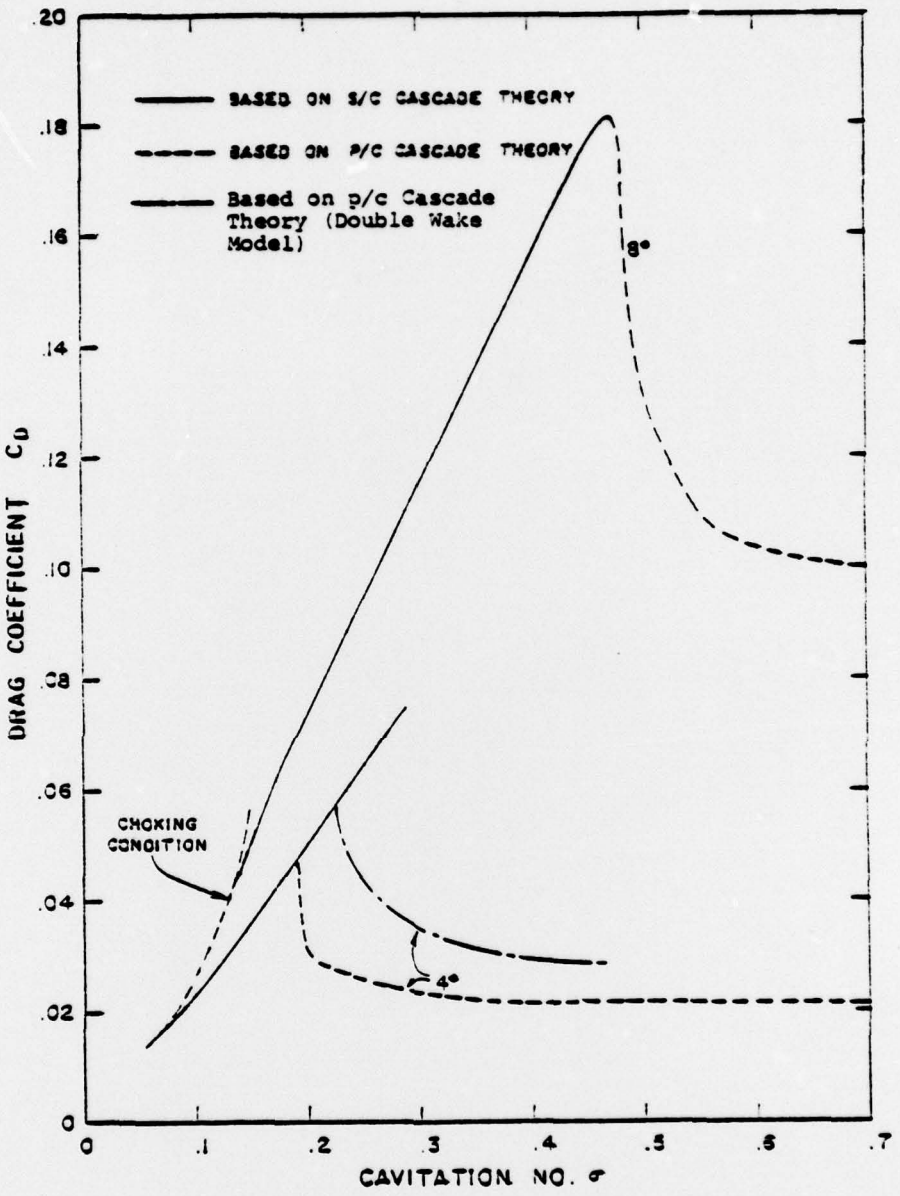

Figure 3.5 Drag Coefficient vs. Cavitation Number for the Same Case as Figure 3.4

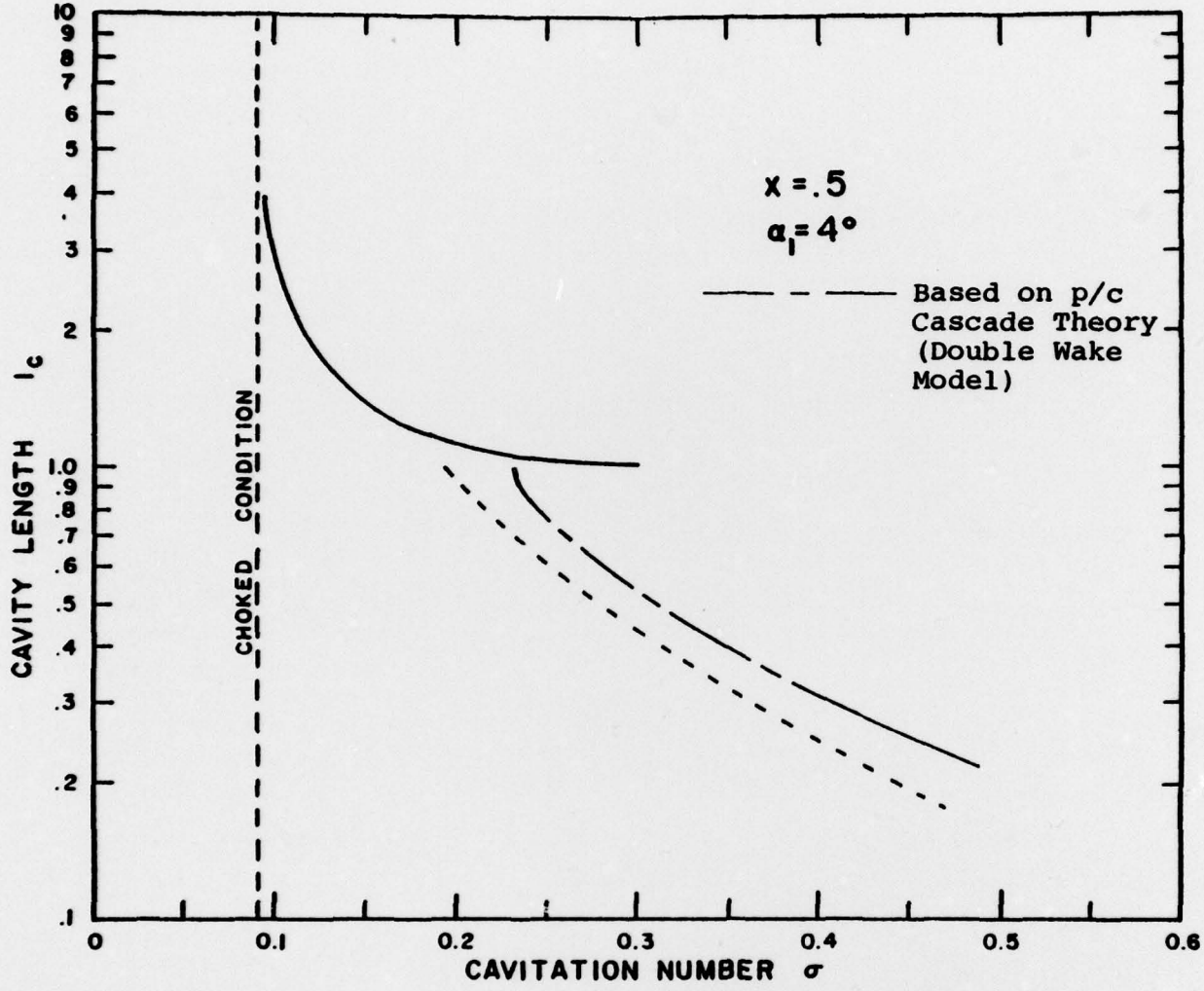

Figure 3.6 Cavity Length vs. Cavitation Number for the Same Case as Figures 3.5 and 3.6